

# Cytodifferentiation in the Accessory Glands of *Tenebrio molitor*.

## VI. A Congruent Map of Cells and Their Secretions in the Layered Elastic Product of the Male Bean-Shaped Gland

PATRICK J. DAILEY, NJIDDA M. GADZAMA, AND GEORGE M. HAPP  
*Department of Zoology, University of Vermont, Burlington, Vermont 05405 (P.J.D., G.M.H.), and Department of Biological Sciences, University of Madaquei, Madaquei, Nigeria (N.M.G.)*

**ABSTRACT** The morphology of the bean-shaped accessory glands (BAGs) of males of *Tenebrio molitor* is described. All cells in the secretory epithelium are long and narrow ( $300\text{--}400\text{ m}\mu \times 5\text{ m}\mu$ ). The seven types of secretory cells are distinguished from one another by the morphology of their secretory granules. Granule substructure varies from simple spheres with homogeneous electron-dense contents to complex forms with thickened exterior walls or with crystalline and membranous contents. Individual cell types were mapped by staining whole glands with Oil Red O, and the cell distributions were confirmed by wax histology and ultramicroscopy. The secretions of all seven cell types form a secretory plug composed of seven layers. During mating, the secretory plug from each BAG is forced into the ejaculatory duct by contractions of a sheath of circular muscle. The mirror image plugs from symmetrical BAGs fuse and are transformed into the wall of the spermatophore.

The accessory glands of insects, like those of vertebrates, promote the transfer of sperm from male to female and the maintenance of viable sperm within the female until fertilization. The roles of accessory glands in insect reproduction (reviewed by Leopold, '76) include: production of a complex spermatophore (Khalifa, '50a, b; Davey, '60), formation of mating plugs (Bishop, '20; Hinton, '64; Labine, '64), sperm activation or capacitation (Bishop, '20; Baccetti, '72; Leopold and Degrugillier, '73), initiation of oviposition (Pickford et al., '69; Riemann and Thorson, '69; Baumann, '74; Jones and Madhukar, '76), and acceleration (sometimes by nutritional contribution) of egg maturation (Abraham, '34; Gillett, '58; Landa, '60, '61; Hinton, '64; Loher and Huber, '66; Judson, '67; Bouletreau, '74).

In some insects, males have a score or more of distinct accessory reproductive glands (Leopold, '76), but in Coleoptera (beetles) only two or three pairs are found. In a meloid beetle,

*Lytta nuttalli*, Gerber ('68) reported that the products of three pairs of tubular glands form the spermatophore. In *Pimelia angulata*, a tenebrionid beetle studied by Fiori ('54), two quite dissimilar pairs of glands are present. The first pair is elongate and tubular, while the second pair is shorter and contains "plastic-like" material that apparently forms the long spermatophore. Similar pairs of glands have been observed in male *Tenebrio molitor* (mealworm beetles) (Khalifa, '49; Davey, '60; Jones, '67; Gadzama, '71; Gerber, '76), where the second pair is kidney bean-shaped. The ultrastructure and adult cytodifferentiation of the tubular glands in *T. molitor* have been examined by Gadzama et al. ('77) and Happ et al. ('77). Preliminary cytological investigations of the bean-shaped glands by Gadzama ('71) suggested that the secretory products of their glands contribute to the spermatophore. Ultrastructural examination of the spermatophore (Gadzama and Happ, '74) and com-

parisons of amino acid compositions and antigens of the bean-shaped gland with those of the spermatophore (Frenk and Happ, '76) yielded data that supported Gadzama's suggestion.

The intent of the present paper is to report the histology and ultrastructure of the bean-shaped accessory glands (BAG) in mature male *Tenebrio molitor*. Secretions from the various secretory cell types contribute to a semi-solid product, the secretory plug. The organization of this plug will also be considered. The morphological cytodifferentiation of these glands in pupae has been described by Grimes and Happ ('80), and a morphological chronicle of adult maturation will be described in a future paper.

#### MATERIALS AND METHODS

Adult males of *Tenebrio molitor* L. were collected at eclosion and maintained on carrot and Purina Chick Startena (Ralston Purina). All our observations were made on virgin males over 8 days of age.

##### *Light microscopy*

Beetles were dissected in phosphate-buffered saline, pH 7.9 (Dulbecco and Vogt, '54), and glands were fixed in 3% glutaraldehyde, or 4% formaldehyde, or alcoholic Bouin's fixative. For staining of whole glands, we used 1% aqueous Trypan blue or 0.5% Oil Red O in aqueous alcohols (60% isopropanol, 99% isopropanol, or 60% ethanol). Glands were then destained and stored in 30% ethanol or 30% isopropanol. For wax histology, glands were dehydrated in an ethanol series, embedded in paraffin, and stained with Harris' haematoxylin or periodic acid-Schiff procedures (Pearse, '68).

##### *Electron microscopy*

Reproductive tracts were removed from beetles in phosphate-buffered saline and immersed in 3% glutaraldehyde (0.1 M phosphate buffer, pH 7.4) for 1–3 hours. During the first hour in the fixative, individual glands were divided into three parts and subsequently fixed for at least an additional hour (Fig. 1). Post fixation was in 1% phosphate-buffered osmium tetroxide for 1 hour. After a quick rinse in distilled water, glands were stained en bloc with 2% aqueous uranyl acetate, dehydrated in a graded acetone series, and embedded in Epon 812. Thick sections were stained in toluidine blue. Thin sections were stained for 20 minutes in 40% uranyl acetate

in methanol followed by 10 minutes in Reynolds' lead citrate (Reynolds, '63). Sections were photographed on a Philips EM 200 transmission electron microscope.

Cross-sectional areas of individual cells of each cell type were determined by tracing the outlines of 15–50 cells of a single type on electron micrographs and then by weighing the paper tracing. Cell heights were measured on low-power micrographs through the epithelium. In order to relate these dimensions of fixed tissues to those of fresh tissue, we have determined that fixation and dehydration of whole BAGs cause shrinkage of 73% of the fresh value (one dimension) or 54% of the fresh value (area).

#### OBSERVATIONS AND RESULTS

The reproductive accessory glands of *T. molitor* originate from the mesodermally-derived vas deferens (Kerschner, '13; Huet, '66; Poels, '72). In the adult male, the BAGs are located in abdominal segment II, slightly anterior to the testes. Each BAG measures about 2.2 mm in length by 1.8 mm in width. The coiled tubular accessory glands, seminal vesicles, and the BAGs converge into the bifurcated, anterior end of the ejaculatory duct in a region referred to as the "Grand Junction" (Fig. 2).

##### *General cell structure*

The secretory cells of BAG are very tall—30–40 times as tall as they are wide. These narrow columnar cells taper gently over their 300–500  $\mu\text{m}$  length from the broader base (near the muscle layer) to a narrower apical surface at the lumen. All the cells share common ultrastructural features: abundant endoplasmic reticulum, numerous Golgi complexes, and many mitochondria. The basal third of each cell contains scattered immature secretory granules, the middle third more numerous secretory granules, and the apical third densely packed secretory granules with few intervening membranous structures. Ovoid nuclei, usually  $11 \times 4 \times 4 \mu\text{m}$ , are aligned with the long axis of the cell in the basal or middle portions (Fig. 12).

Intercellular junctions between homologous and heterologous cell types are of the continuous form (zonula continua) (Fig. 21). The intercellular space between adjacent membranes is 123 Å, which is very similar to junctions found in *T. molitor* larval intestinal epithelium by Noirot and Noirot-Timothee ('67). As continuous junctions approach the cell apex, dense material is formed at the

		<i>Abbreviations</i>			
BAG	bean-shaped accessory gland	L	lumen	RER	rough endoplasmic reticulum
BD	belt desmosome	LG	lacework granule	SER	smooth endoplasmic reticulum
CJ	continuous junction	LM	limiting membrane	SV	seminal vesicle
EJD	ejaculatory duct	LS	lucent space	T	testis
FG	faceted granule	M	mitochondrion	TAG	tubular accessory glands
GC	Golgi complex	MG	multivesicular granule	TC	tubular convolutions
GJ	grand junction	MT	microtubule	TG	thick-walled granule
GM	granule matrix	N	nucleus	VD	vas deferens
GW	granule wall	P	plug	VG	vesicular granules
		R	ribosomes		

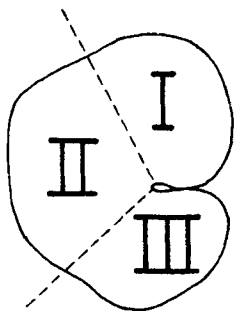


Fig. 1. Illustration showing dissection of the BAG into three parts prior to embedding for electron microscopy.  $\times 16$ .

inner surface of each membrane. These electron-dense regions are characteristic of belt desmosomes or zonulae adhaerentes (Satir and Gilula, '73) (Fig. 21).

The apical cytoplasm of each cell type possesses numerous microtubules (Figs. 15, 29, 49). These microtubules generally lie parallel to the long axis of the cell. Electron micrographs suggest that microtubules also traverse cell membranes between homologous cell types (Figs. 29, 49). Noirot-Timothee and Noirot ('66) have reported that epithelial cell microtubules of the foregut and hindgut of termites insert at specific attachment zones on the plasma membrane.

The secretory granules are not uniformly packed throughout the apical portions of these cells. Near to the gland lumen is a well-defined apical zone, free of most secretory granules and appearing as a "halo" around the lumen in light micrographs (Fig. 8A). This zone of granule exclusion varies in width and contains microtubules, a few mitochondria, and relatively few secretory granules. The zone of exclusion lies at the level where cells are closely bound to one another by continuous junctions (Fig. 8A). Adjacent to the apical surface is a narrow band of secretory granules,

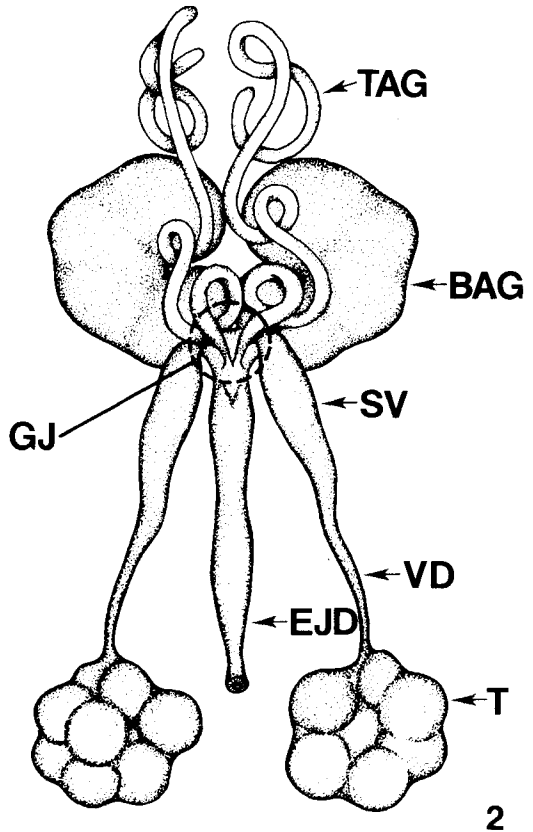


Fig. 2. Male reproductive system *T. molitor*. Tubular accessory gland (TAG), bean-shaped accessory gland (BAG), seminal vesicle (SV), vas deferens (VD), ejaculatory duct (EJD), testis (T), and grand junction (GJ).  $\times 13$ .

and basal to the zone of exclusion, the secretory granules are closely packed (Figs. 12, 13). This zone of granule exclusion is unlikely to be a fixation artifact, since it is seen after a variety of fixatives in both light and electron micrographs.

Wax sections stained with haematoxylin and thick Epon sections stained with toluidine

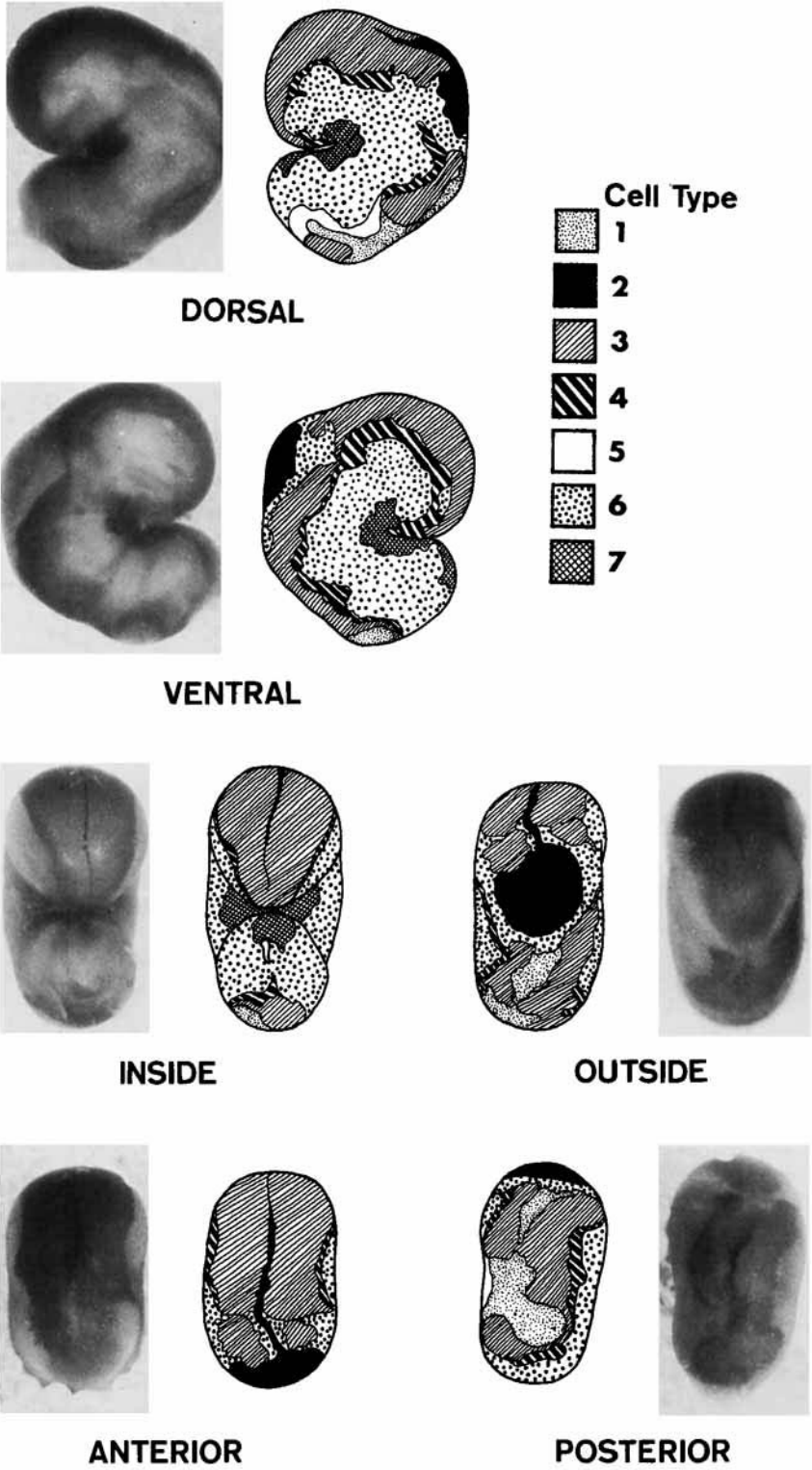


Fig. 3. Patterns of distribution of seven cell types in the male bean-shaped accessory gland of *T. molitor* in Oil Red O-stained glands.  $\times 15$ .

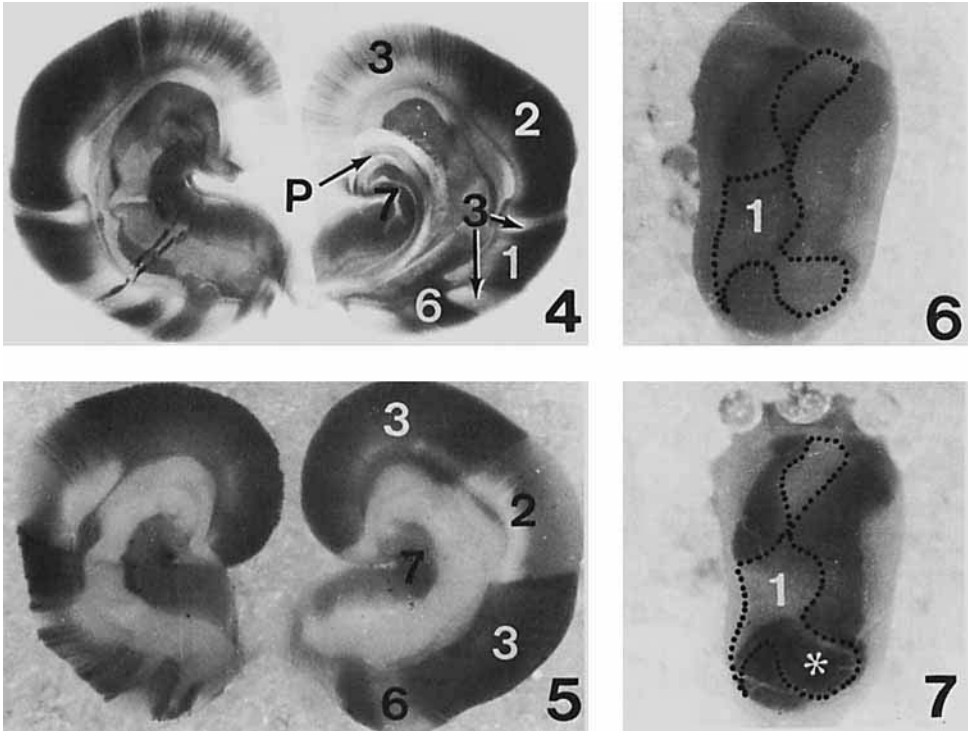


Fig. 4. Internal views of the dorsal (left) and ventral (right) halves of the BAG after staining with trypan blue. The secretory plug (P) has been lifted from the gland lumen and shifted slightly to the left. Note how closely the plug shape conforms to that of the lumen. Numbers correspond to cell type regions.  $\times 24$ .

Fig. 5. Same view as Figure 4; however, gland stained in Oil Red O.  $\times 24$ .

Fig. 6. Posterolateral surface of bean-shaped accessory gland after staining in a 99% isopropanol stain of Oil Red O for 24 hr. Stippled boundary indicates region occupied by cell type 1.  $\times 24$ .

Fig. 7. Posterolateral surface of bean-shaped accessory gland after staining in 60% isopropanol solution of Oil Red O for 24 hr. Asterisk (\*) indicates portion of region 1 (cell type ) that stains geranium red in 60% solution. This particular area becomes pink when the gland is placed back into 99% isopropanol stock solution and cannot be distinguished as a separate region therein. Compare with Figure 6.  $\times 24$ .

blue revealed dramatic differences in the basophilia and metachromasia of different patches of cells. Heterogeneously staining cells are not mixed together in a salt-and-pepper pattern. Individual cells do not lie as islands in a sea of heterologous cells. Instead, each staining type forms a cohesive mass, and sharp boundaries fall between the patches of dissimilar cells (Figs. 8, 9, 23). Electron microscopy showed that the secretory granules of the heterologous cells are sharply different. Heterogeneity of the secretory granules of BAG and the complex shapes of the patches of each cell type complicated our early attempts to define the characteristics of the various morphological phenotypes and to map their

distributions on the surface of the BAG. However, we were able to develop a coherent map of the BAG surface by a combination of stained whole mounts, wax histology and serial sections, thick Epon sections, and electron microscopic examination of precisely defined regions of the BAG.

Whole glands were fixed in glutaraldehyde and stained in toto. Oil Red O partitioned the gland into regions rich in lipids, and trypan blue revealed particularly high concentrations of protein. Trypan blue showed a protein-rich zone along the lateral margin of the BAG and other protein-rich areas on the dorsal and ventral surface. Some zones did not stain blue but remained white. The same pattern of

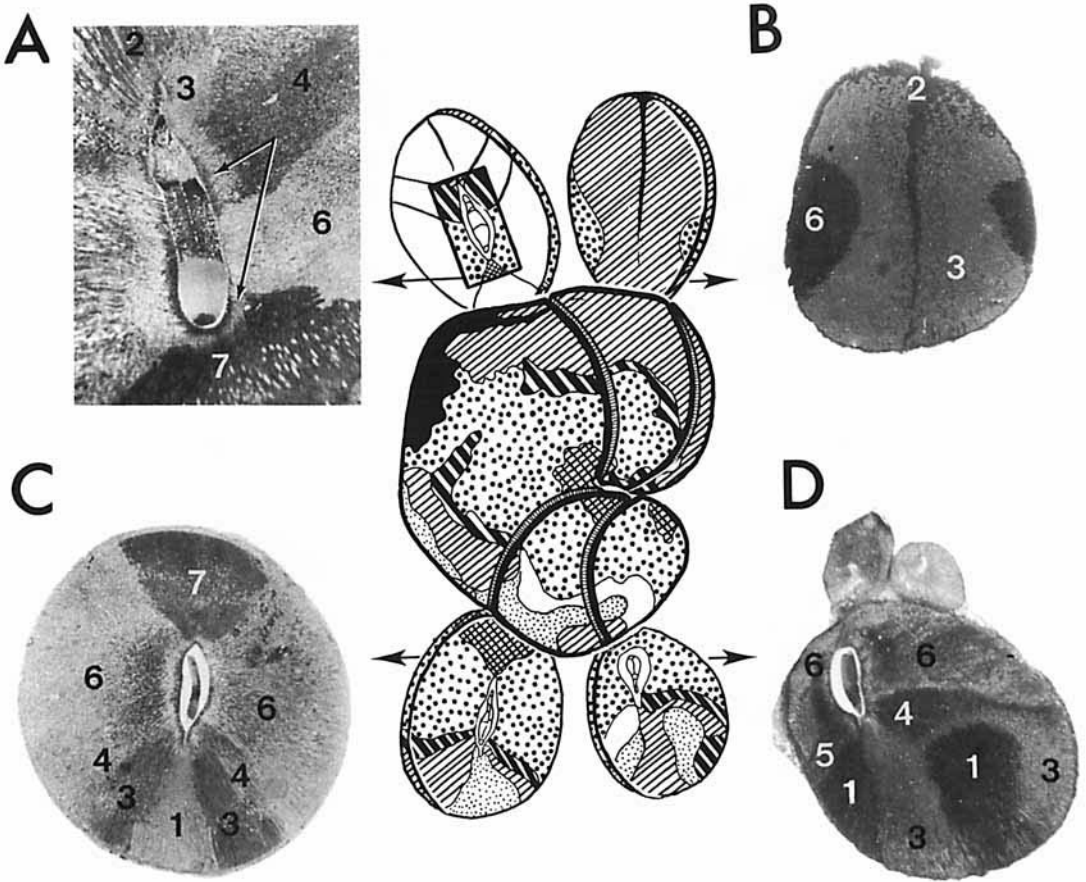


Fig. 8. Three-dimensional representation of the BAG. Photographs of toluidine-blue stained, thick Epon sections can be easily understood if they are conceived of as discs slid out of the three-dimensional gland. Arrow in A shows zone of granule exclusion. Symbol conventions as in Figure 3. A,  $\times 80$ ; B,  $\times 45$ ; C,  $\times 47$ ; D,  $\times 50$ .

white and blue patches were stained consistently in a series of glands processed in parallel. In a complementary staining series, the zones with low affinity for trypan blue showed a high affinity for Oil Red O. A careful examination of the glands stained with Oil Red O allowed us to distinguish consistently seven different hues or intensities, ranging from clay-colored to scarlet. These colors have been described below according to the system in Smithe's ('75) *Naturalists' Color Guide*. Each of the seven distinct colors was found in the same patchy distribution on each BAG. Each of the seven colors comprises a homogeneous secretory cell population, and each of these seven cell types has secretory granules with a unique, characteristic ultrastructure (Fig. 11). By examining many samples of Oil Red O stained BAGs in the stereomicroscope, we

were able to map the seven cell types as viewed from every aspect. Both photographs and drawings of these aspects are shown in Figure 3. The staining pattern was also seen in glands that have been split to expose the lumen (Figs. 4, 5).

Once we had constructed the surface map, it was rather easy to trace each cell type from the outer surface to the gland lumen and thus to decipher the sectioned material (Figs. 8, 9).

The camera lucida projections of each patch of cells were traced upon a 50:1 three-dimensional plasticene model of the BAG. Then this scale model was xeroxed from many angles to provide 50:1 xerox tracings of each differently staining patch. The area occupied by each cell type was determined by weighing the tracings (Fig. 10A). Mean basal cross-sectional areas of each individual cell type were determined by

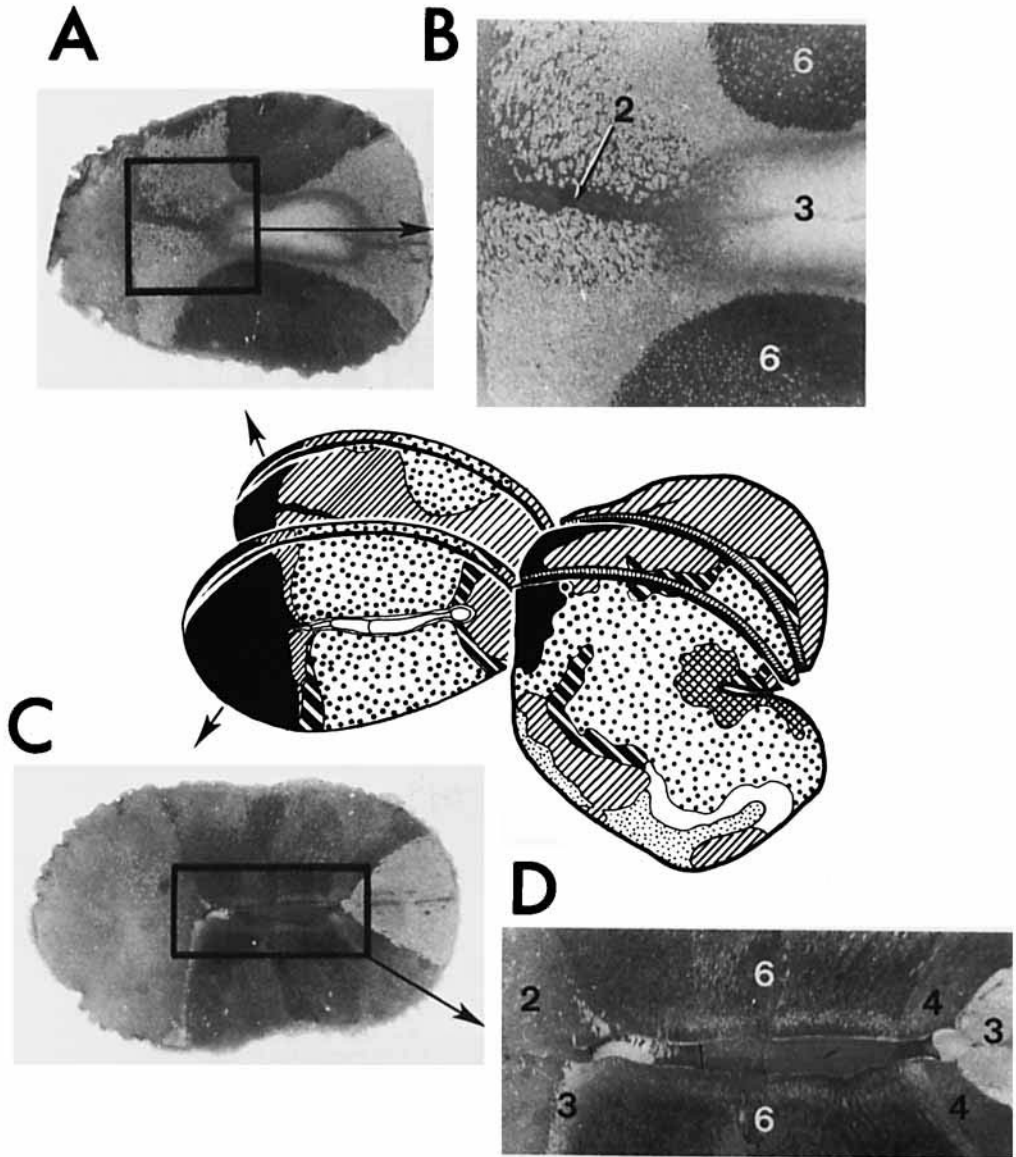


Fig. 9. Three-dimensional representation of the BAG, as shown in Figure 8. Note especially the narrow tongue of type 2 cells (arrow in B) and the plug in D. A,  $\times 50$ ; B,  $\times 134$ ; C,  $\times 48$ ; D,  $\times 124$ .

weighing tracings from appropriate electron micrographs (Fig. 10C). The mean length of each cell type was also measured (Fig. 10B). By dividing area per cell (Fig. 10C) into epithelial area per cell type (Fig. 10A), we calculated the numbers of each cell type (Fig. 10D). By summation of values for the seven types, we found the total surface area of the gland to be ca. 6 mm<sup>2</sup> and the total number of cells to be about 200,000 per BAG.

In order to distinguish among the various

cell types, refer to Figure 11 for a simplified drawing of the most common secretory granules and to Table 1 for their dimensions. As will be shown below, the numbering convention is based on the layering of the secretory products with the secretory plug.

*Cell type 1*

Cell type 1 is found in the posterolateral region of the BAG, which stains pink with Oil Red O (Fig. 3) and has a high affinity for

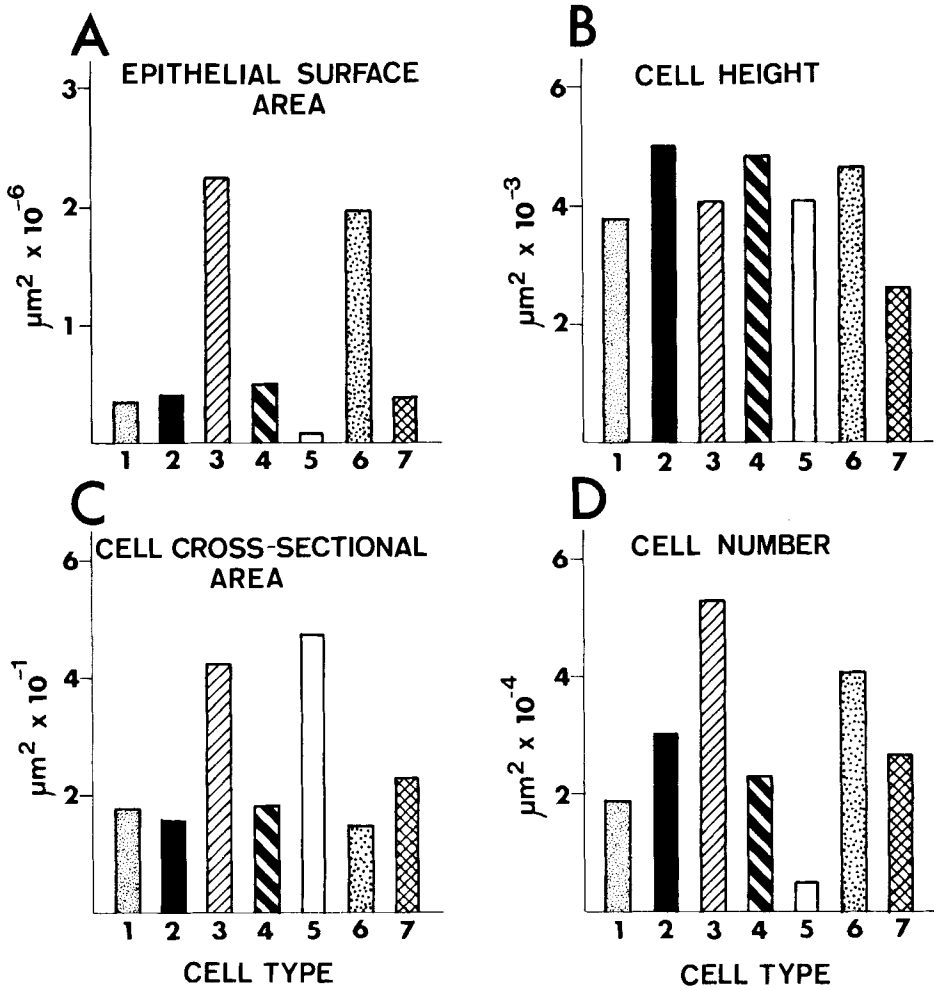


Fig. 10. Quantitative description of epithelial cell types 1-7. A) Epithelial area for each cell type (1-7). B) Mean cell height determined by measurement on electron micrographs of at least ten cells of each type and corrected for shrinkage. C) Mean cell cross-sectional area measured by tracing the outlines of individual cells (20-50 of each type), weighing the tracings, and correcting for shrinkage. D) Cell number was determined by dividing epithelial area (A) by cell cross-sectional area (C). Horizontal axis represents cell type.

toluidine blue (Figs. 8C, D). Most profiles of endoplasmic reticulum are ribosome-studded (Fig. 14). Globular secretory granules have an electron-lucent center and an electron-dense cortex (Figs. 14, 15, 19). Many of the granules appear to originate in the Golgi (Figs. 14, 18), and as the granules mature and approach the lumen, the many small electron-lucent spheres appear to fuse to yield simpler granules with fewer and larger electron-lucent areas (Figs. 14, 19, 21, 22). When viewed in tangential section through the wall, the peripheral structure of these granules appears as a network of dense material with intervening spaces (Fig.

16). Some granules apparently fuse to yield very large masses (Fig. 17). When secreted into the lumen, the type 1 granules form frothy masses (Fig. 22).

Simple granules might also arise by transformation of mitochondria (Figs. 19, 20). Electron micrographs suggest that mitochondria become barbell shaped and that the two bulbous ends bend toward each other and fuse.

The most posterior cells of the type 1 patch have a higher affinity for Oil Red O than do the other type 1 cells (Figs. 6, 7). This is also true of EM thick sections stained with toluidine blue. In these the posterior aspect of the

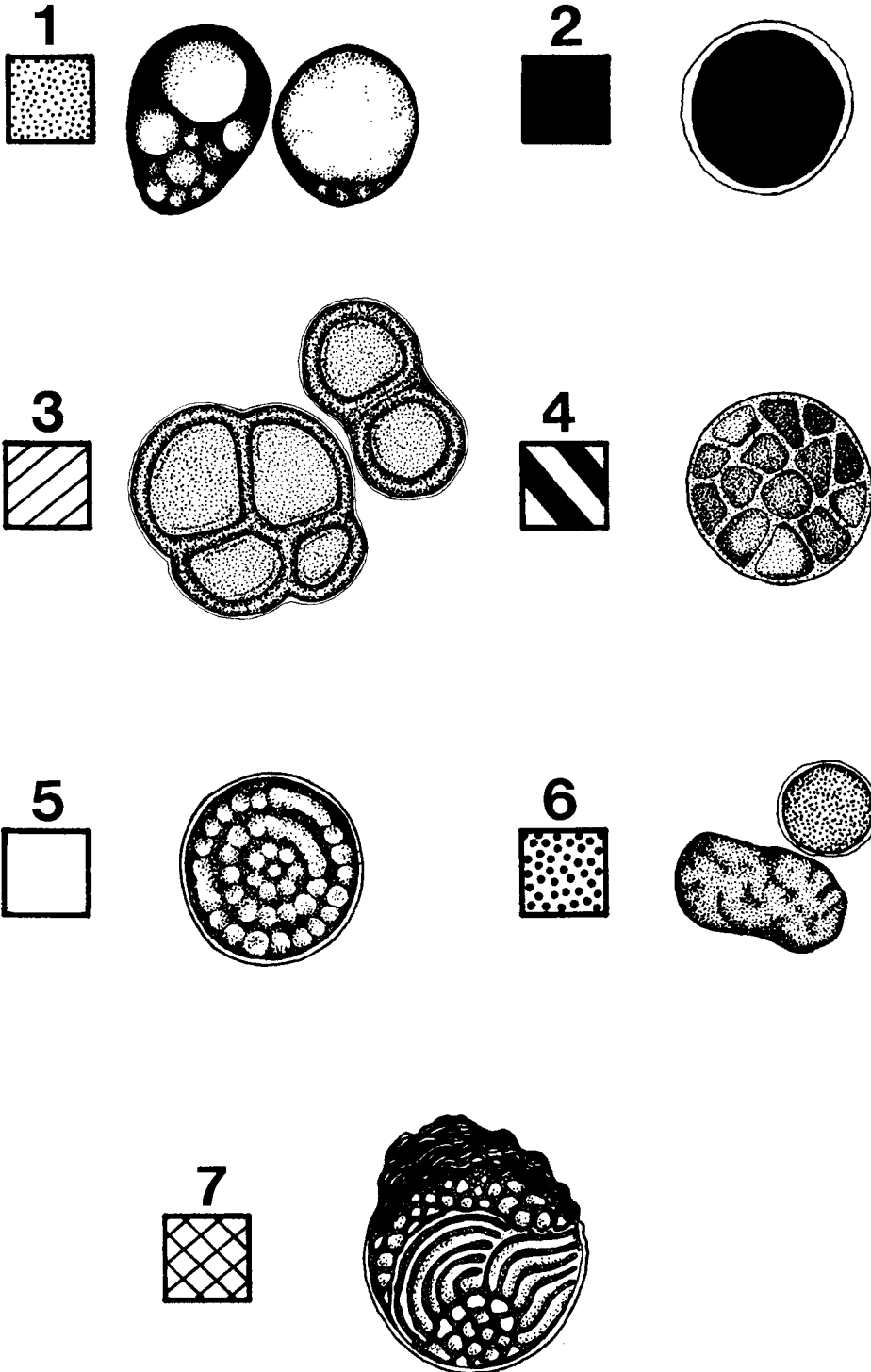


Fig. 11. This illustration depicts the ultrastructural morphology of the most common secretory granules synthesized by the seven epithelial cell types of the bean-shaped accessory gland. Drawings were made from electron micrographs  $\times 25,000$ .

TABLE 1. Granule classification and dimensions within specific cell types observed in BAG

Cell type	Granule class	Dimensions ( $\mu\text{m}$ )	
		Length	Width
1	Globular	$0.8 \pm 0.3^*$	$0.7 \pm 0.2$
2	Simple	$0.7 \pm .01$	$0.6 \pm .09$
	Paracrystalline	$2.7 \pm 1.6$	$1.7 \pm 0.7$
3	Thick-walled	$1.3 \pm 0.1$	$0.8 \pm 0.1$
	Thick-walled		
	Rod-bearing	$0.6 \pm 0.2$	$0.4 \pm 0.1$
	Lacework	$3.1 \pm 1.1$	$2.2 \pm 0.7$
4	Faceted	$0.5 \pm 0.2$	$0.4 \pm 0.2$
5	Concentric	$0.7 \pm 0.1$	$0.6 \pm 0.1$
6	Simple	$0.8 \pm 0.2$	$0.7 \pm 0.1$
7	Multitubular	$0.6 \pm 0.1$	$0.5 \pm 0.1$
	Complex	$1.2 \pm 0.2$	$1.0 \pm 0.2$

\* Standard deviation.

region occupied by cell type 1 stains intensely basophilic, whereas the anterior aspect stains lightly basophilic (Figs. 8C, D). Electron micrographs show that these cells contain more of the simple granules with single, large, electron-lucent spaces and thick, outer electron-dense shells than do the surrounding cells.

#### Cell type 2

After Oil Red O staining, a round clay-colored patch of type 2 cells is evident on the lateral margin of the BAG. From this circular patch a narrow tongue of type 2 cells runs forward to the anterior tip of the BAG (Fig. 9A, B). These cells are intensely basophilic with both haematoxylin and toluidine blue. Although they contain much rough endoplasmic reticulum, some smooth membrane profiles are present, especially near the Golgi. Most (80–90%) of the secretory granules are spherical with electron-dense centers that

often shrink away from the bounding membrane (Figs. 24–26). A few of the granules are angular (sometimes even hexagonal) and contain a closely spaced system of parallel membranes (Fig. 27), each about 5 nm in thickness, with a periodicity of 14 nm. These granules, termed paracrystalline, are much larger than the spherical variety (Fig. 24).

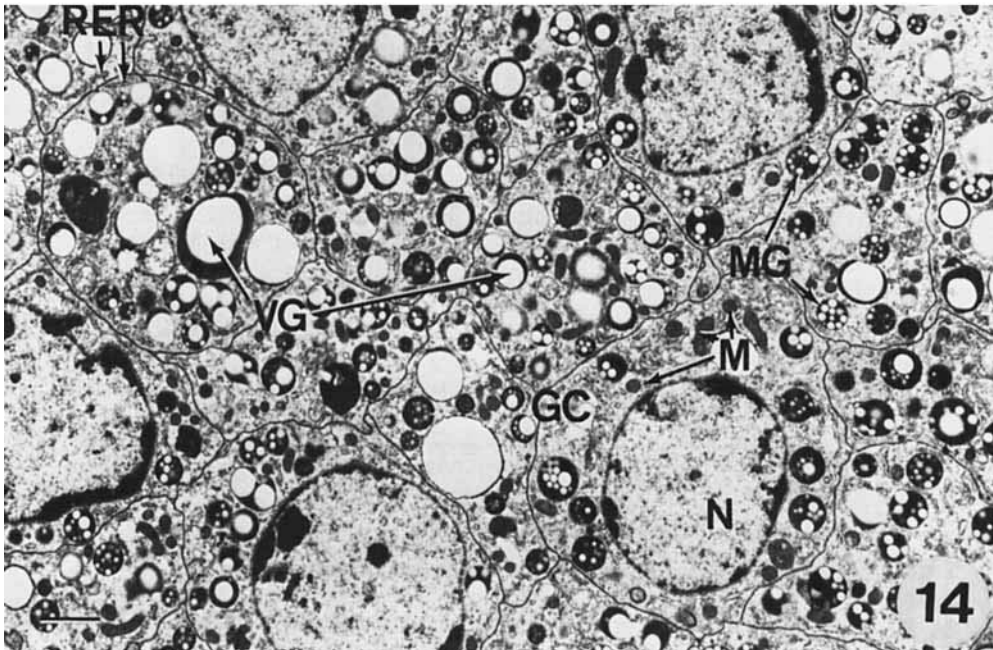
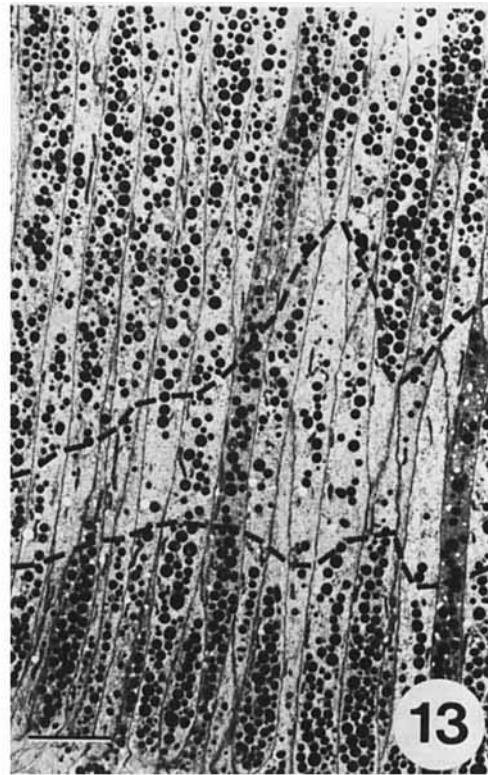
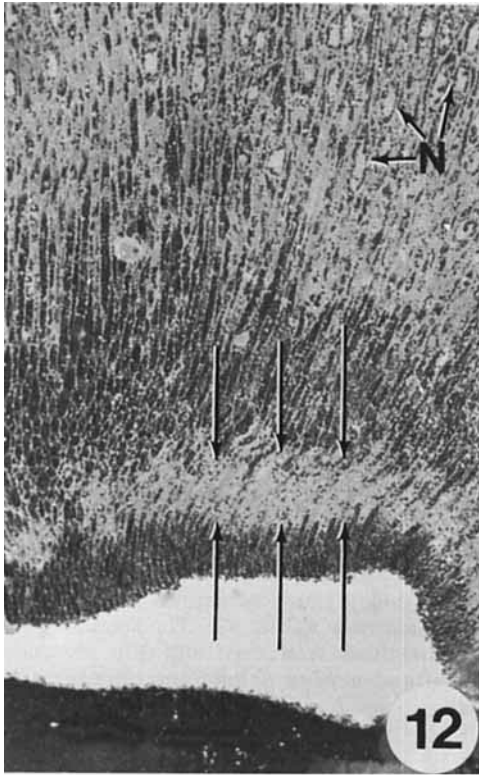
#### Cell type 3

Type 3 cells are bright scarlet in whole mounts stained with Oil Red O (Fig. 3) and stain a pale green with toluidine blue (Figs. 8, 9). Rough endoplasmic reticulum is uncommon, and smooth membrane profiles predominate (Fig. 28). Granules are of the two basic kinds: thick-walled and lacework (Figs. 29, 31). The thick-walled granules are most numerous. They originate from the Golgi (Fig. 30), and their peripheral structure is complex. The wall is not a simple unit membrane. The

Fig. 12. Light micrograph demonstrating zone of granule exclusion (between arrows) above the apical cell surface. Another dense granular zone similar to that at the apical surface occurs immediately above the zone of exclusion. Longitudinal sections through cell nuclei (N) are also evident.  $\times 900$ .

Fig. 13. Electron micrograph depicting the zone of granule exclusion. Note that the exclusion zone is not as sharply defined as in Figure 12. Dashed lines indicate rough boundary of granule exclusion zone. Bar = 5.0  $\mu\text{m}$ .

Fig. 14. Transverse section through type 1 cells. Note the diverse morphology of multivesicular granules (MG). Other inclusions are vesicular granules (VG), rough endoplasmic reticulum (RER), Golgi complex (GC), mitochondria (M), and cell nucleus (N). Bar = 1.0  $\mu\text{m}$ .



outer limiting membrane is 7.5 nm in thickness and consists of two dense lines separated by an electron-transparent zone (3 nm in thickness). Beneath this limiting membrane is a thick cortex consisting of short, radially-directed electron-dense ribs alternating with electron-transparent spaces (Figs. 32, 33, 37). In tangential sections, the array of electron-dense and lucent spaces appears as an array of closely packed vesicles (Fig. 32). In many granules the wall invaginates and divides the medulla of the granule into several compartments (Fig. 31). Some thick-walled granules are ellipsoid and contain large rod-like structures (Fig. 35).

Lacework granules are larger and have heterogeneous electron-dense contents, which include tubular masses, granules, and paracrystalline inclusions (Figs. 34, 36).

#### *Cell type 4*

After staining of BAG with Oil Red O, a narrow vinaceous (burgundy red) band runs between type 3 and type 6 cells (Fig. 3). These cells are moderately basophilic (Figs. 8D, 9C, D). The type 4 cells contain multiply-divided granules that are faceted in cross section. These granules appear to arise near the Golgi as membrane-bound spaces containing clumped, spherical dense masses (Fig. 39). The spherical masses grow gradually larger, and the spaces between them become filled with a fine granular material (Fig. 38). Some of the granule contents are fixed as concentric lamellae, and similar lamellae are found in homologous granules in the gland lumen (Fig. 40).

#### *Cell type 5*

On the dorsal surface of the glands, a small, narrow zone between cell types 3 and 6 stains

a salmon color with Oil Red O; it is composed of cell type 5 (Fig. 3). This cell type occupies a position analogous to that of cell type 4, but unlike type 4, these cells are large (Fig. 41) and the secretory granules are not faceted. When photographic exposures are correct for the endoplasmic reticulum, the granule contents appear uniformly dense (Fig. 41). But when shorter exposures are made, the granules are seen to contain many electron-transparent spaces, apparently spherical and ca. 70 nm in diameter (Figs. 42–44). As the granules mature, the contents become arranged in spirals or in bull's-eye patterns (Figs. 45, 46).

#### *Cell type 6*

A major portion of the dorsal and ventral surfaces of BAG is occupied by cell type 6, which is flesh-colored in whole glands stained with Oil Red O (Fig. 3), and lavender in sections stained with toluidine blue (Figs. 8, 9). The cytoplasm of these cells is packed with rough endoplasmic reticulum and many central Golgi zones (Fig. 47). The secretory granules originate from the Golgi (Fig. 48) and are usually somewhat oblong and angular in outline.

#### *Cell type 7*

Cell type 7, which is found on the inner curve of BAG, stains a ferruginous (rusty) red with Oil Red O (Fig. 3). This cell type is characterized by unusually complex secretory granules that contain a variety of membranous lamellae, whorls, tubules, etc. (Figs. 50–54).

#### *The secretory plug*

The lumen of the BAG in an unmated mature male is filled with elastic material, the

Fig. 15. Apical region of type 1 cells. Microtubules appear to extend between cells in regions of cell contact (arrows). Bar = 1.0  $\mu\text{m}$ .

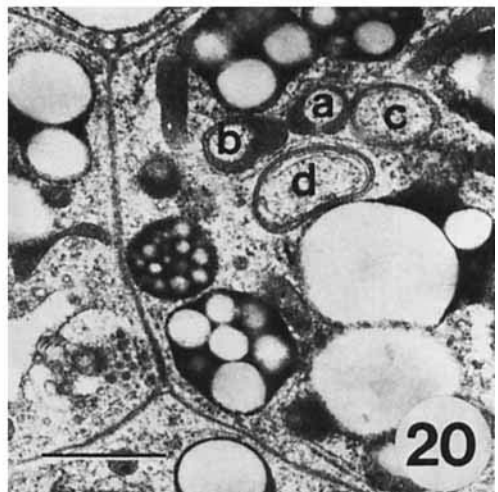
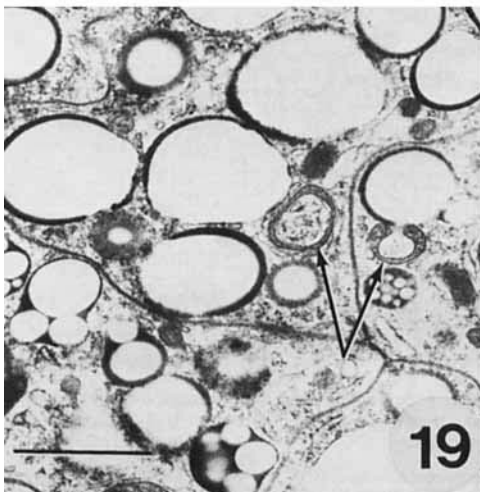
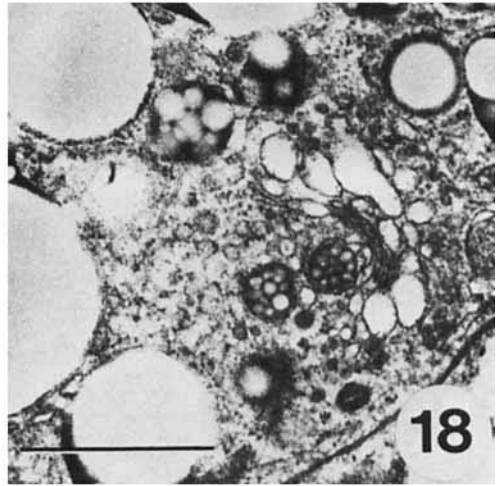
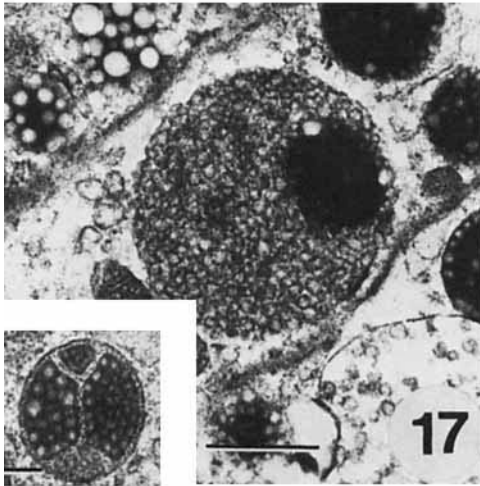
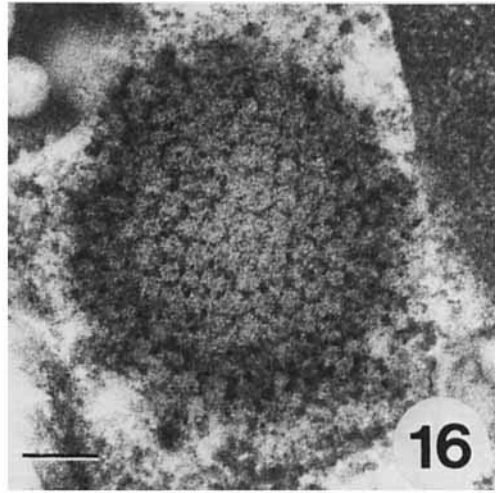
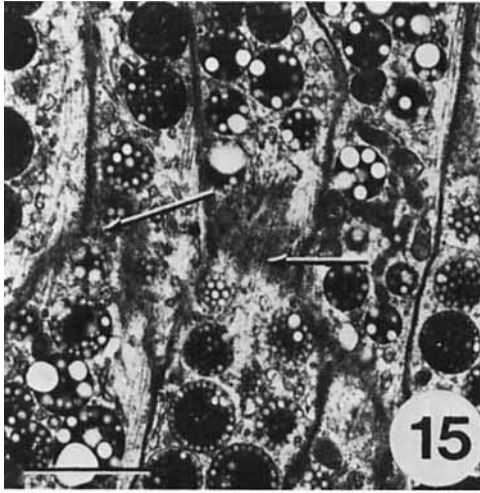
Fig. 16. Section through granule surface demonstrating pattern of small granules forming a mesh-like network. Note cross section through granule at upper left corner. Bar = 1.0  $\mu\text{m}$ .

Fig. 17. Large granular mass containing clear spaces of similar size that have not coalesced. These granules were not frequently observed (bar = 0.5  $\mu\text{m}$ ). Inset demonstrates compartmentalization of granule (bar = 0.2  $\mu\text{m}$ ).

Fig. 18. Golgi complex of cell type 1. Bar = 0.1  $\mu\text{m}$ .

Fig. 19. Several "transforming mitochondria" (arrows) are seen in this micrograph. Bar = 1.0  $\mu\text{m}$ .

Fig. 20. Sequence of possible mitochondrial transformation. The mitochondrion first becomes barbell-shaped (a), the bulbous ends fuse, encompassing some of the cell cytoplasm (b), and eventually the chondriosome membrane becomes equally wide throughout (c) and (d). The contents of transformed mitochondria are similar to those of the surrounding cytoplasm but may appear more flocculent in some cases. Bar = 1.0  $\mu\text{m}$ .



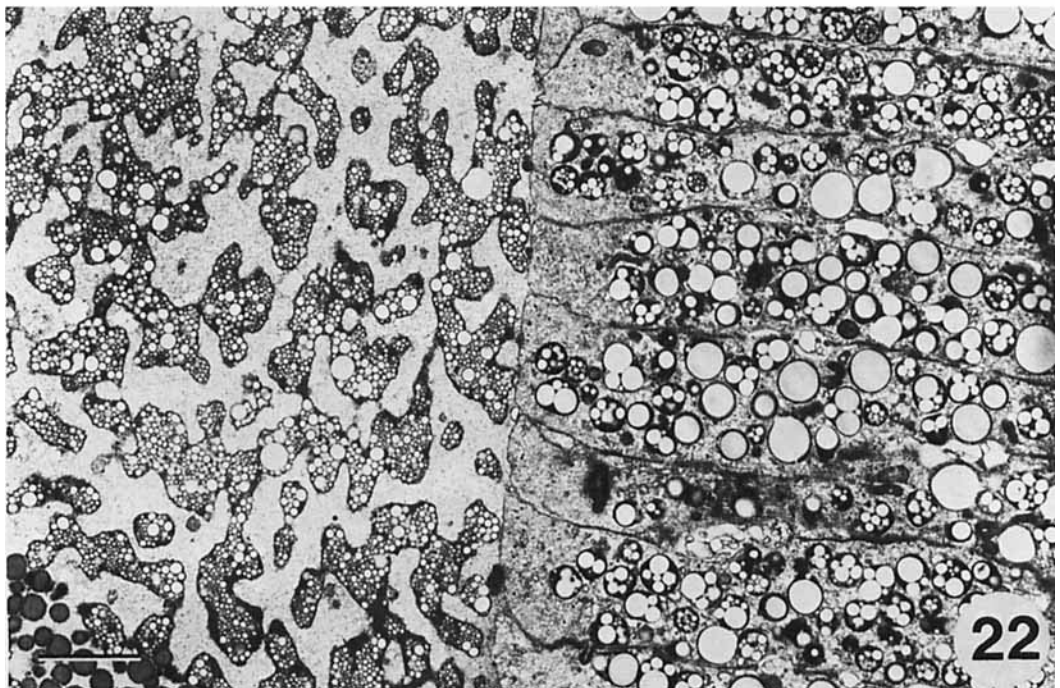
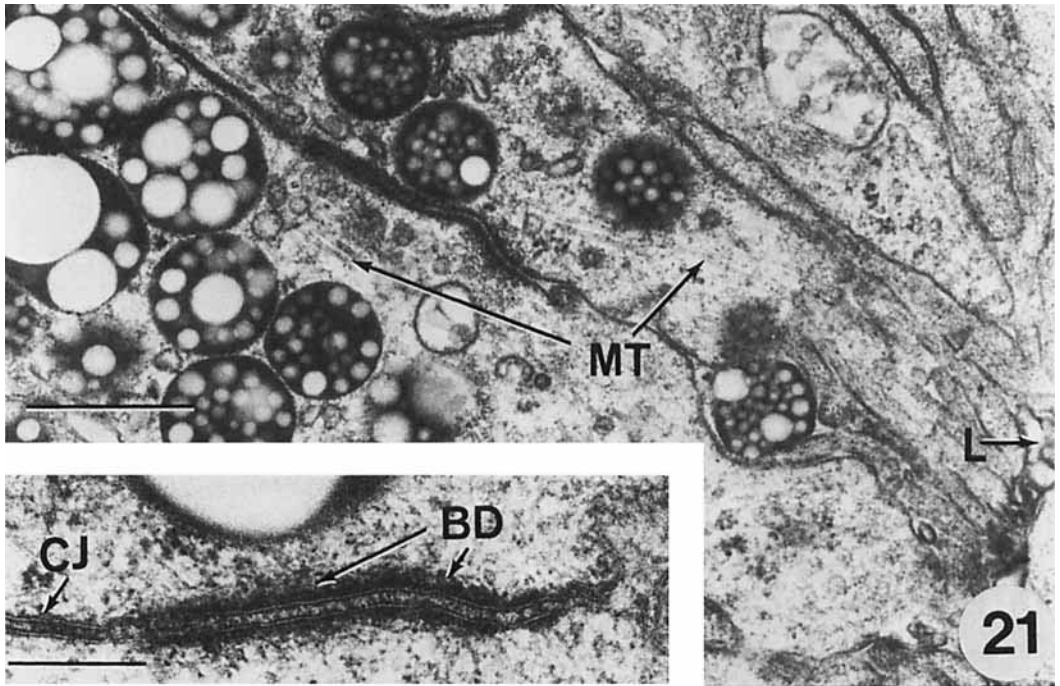


Fig. 21. Apical region of cell type 1 with characteristic electron-dense belt desmosomes marking the regions of cell contact. Inset illustrates continuous junctions (CJ) between cells that become modified to form belt desmosomes (BD) at the apical region. Microtubules (MT), gland lumen (L), Bar = 0.5  $\mu$ m.

Fig. 22. Apical border of cell type 1 adjacent to gland lumen containing frothy, multivesiculate secretory product of these cells. Secretory product of cell type 3 can be seen at the lower left corner of the micrograph. Bar = 2.0  $\mu$ m.

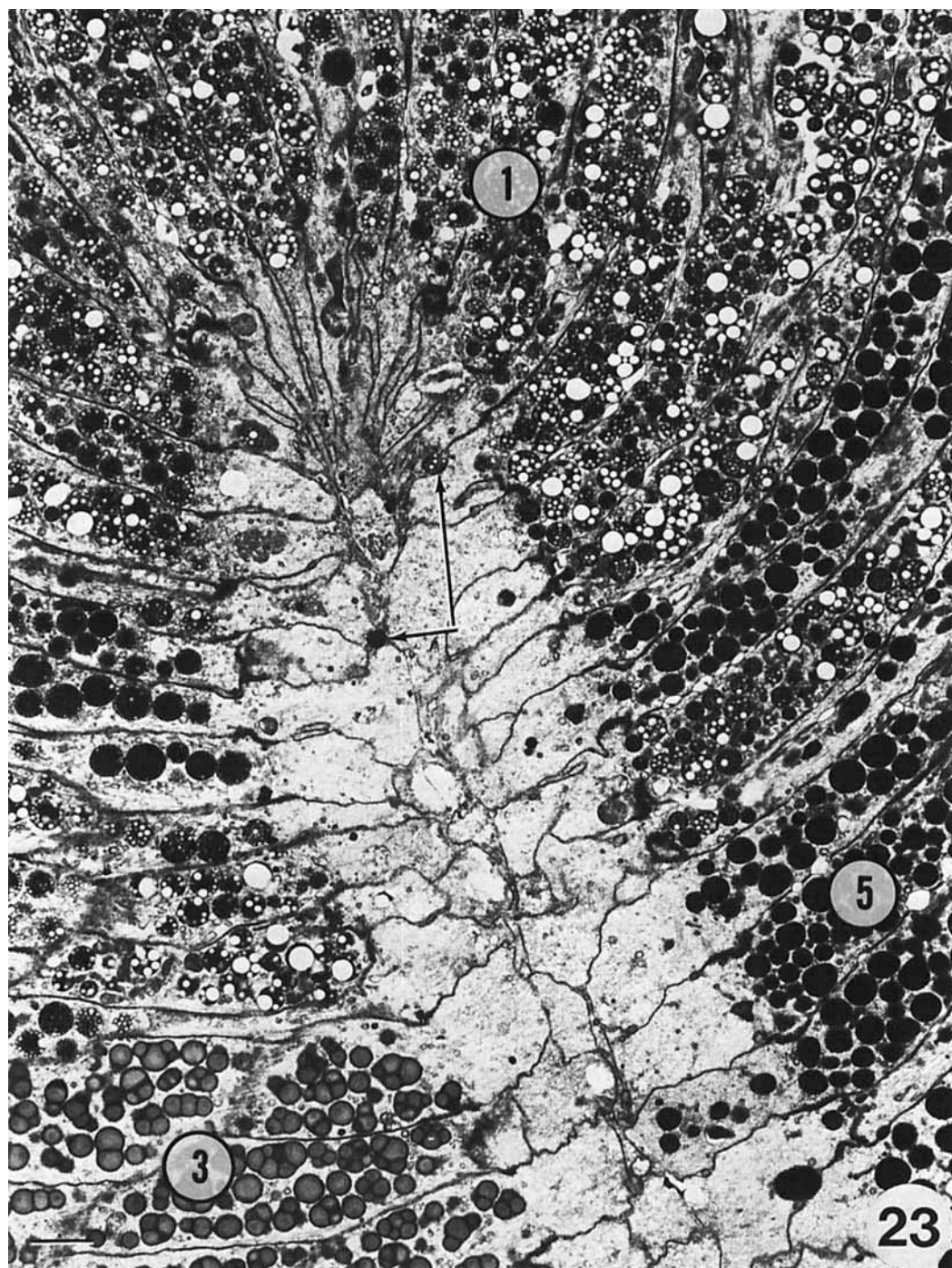


Fig. 23. Several cell types bordering each other. Cell types are, from left to right: 3, 1, and 5. Multilobed granules are characteristically observed in the apical region of cell type 3. Bar = 1.0  $\mu$ m.

secretory plug. The plugs can be removed from fresh glands by gently pulling upon the ejaculatory duct. As the plugs exit the glands, they are elongate, elastic, and sticky. In fixed material, the plugs are inelastic and appear hook-shaped, following the contours of the lumen of BAG (Figs. 4, 58).

The secretory plugs are ordered structures. The various types of secretory granules do not mix into a homogeneous mass. Instead, the products of each cell type form a coherent layer, which can be demonstrated with appropriate stains (Figs. 55–57) in light micrographs as well as in electron micrographs (Figs. 62–66). In order for the layers to be formed with such precision, the cells must secrete in a coordinated manner, and, in fact, the cells are distributed properly to give rise to the ordered plug. One can map the seven cell types with an Eckert projection (Fig. 67), which emphasizes the approximate center of symmetry down the outside curve of the BAG. From type 1 at the center, the zones proceed outward in numerical order. Cell types 1 and 2, on the outer margin of the BAG (Fig. 67), produce the outer layer of the plug (Fig. 68), while cell type 7, on the inner margin of the BAG (Fig. 67), produces the innermost layer of the plug (Fig. 68). The intervening layers are also in sequence.

Plugs from the two glands fuse as they enter the ejaculatory duct (Fig 59), but once again the fusion is ordered so that only homologous layers join with one another (Figs. 60, 61). This phenomenon is shown diagrammatically in Figure 69. The placement of the layers at the grand junction is *not* like that in the wall of the spermatophore, and the process of reorganization of these materials into the spermatophore wall is under investigation.

#### DISCUSSION

The design of the bean-shaped accessory glands allows the production of an organized, layered secretory plug, which is subsequently

transformed into the wall of the spermatophore. Each layer of the plug is derived from secretory granules of a particular cell type, and the seven cell types are distributed in coherent masses with precise boundaries. Such sharp boundaries are common in pigment patterns and at the edges of developmental compartments found in *Drosophila* ectoderm (Crick and Lawrence, '75) but are not commonly known in mesodermally-derived epithelia. The assignment of cell lineages (or polyclones?) to one patch or another and the shaping of each patch are intriguing developmental problems that we will not discuss further at this time. However, we will concern ourselves with two interesting aspects of the BAG, the diversity of secretory granules therein and the formation of organized layers of secretion as a general phenomenon in insect development.

#### *Diversity of secretory granules*

In BAG, as in most exocrine secretory systems, both the endoplasmic reticulum and the Golgi are involved in the formation of the membrane-bound primary secretory granule. The maturation of each type of granule continues as it traverses the hundred microns or more between Golgi and the cell apex. When one surveys the voluminous literature on the ultrastructure of secretion, the detailed variation in secretory granules seems endless. Probably some of the variation is due to differences in fixation among investigators, among tissues, and among positions in the piece of fixed tissue (at the surface or in the interior). However, the consistent similarities in granule morphology in each of the cell types of BAG and the consistent differences among the cell types, all of which are fixed simultaneously, preclude an artifactual explanation of the diverse morphology.

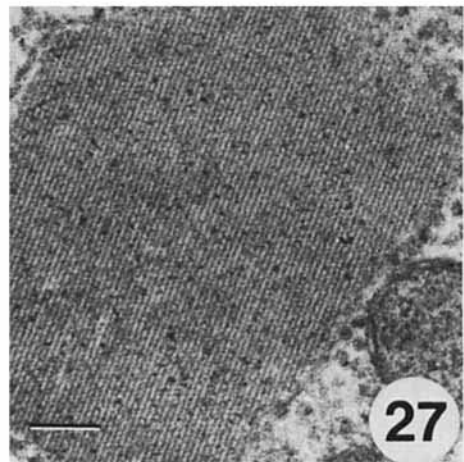
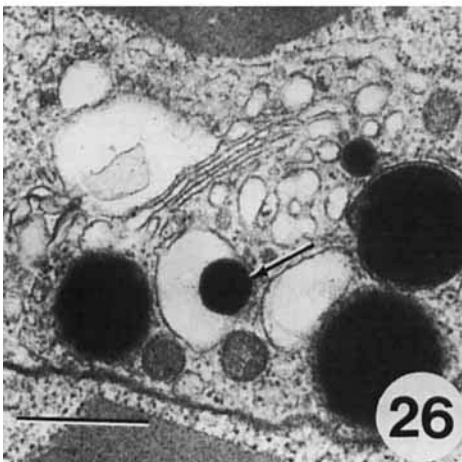
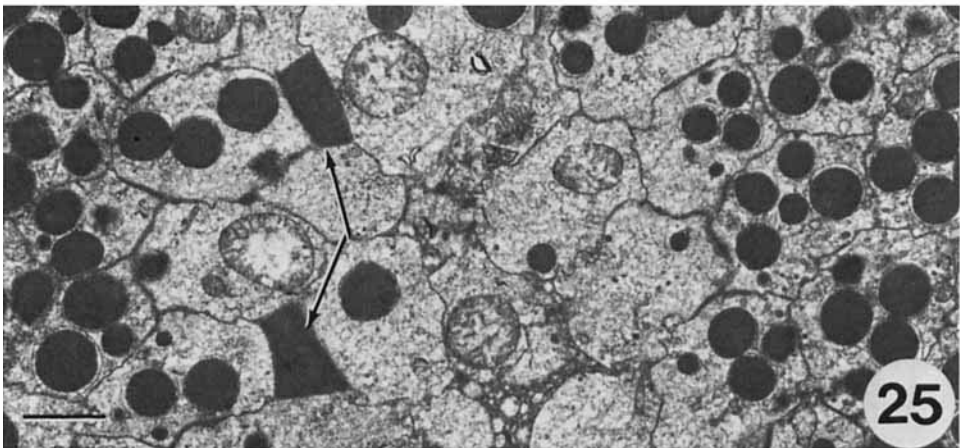
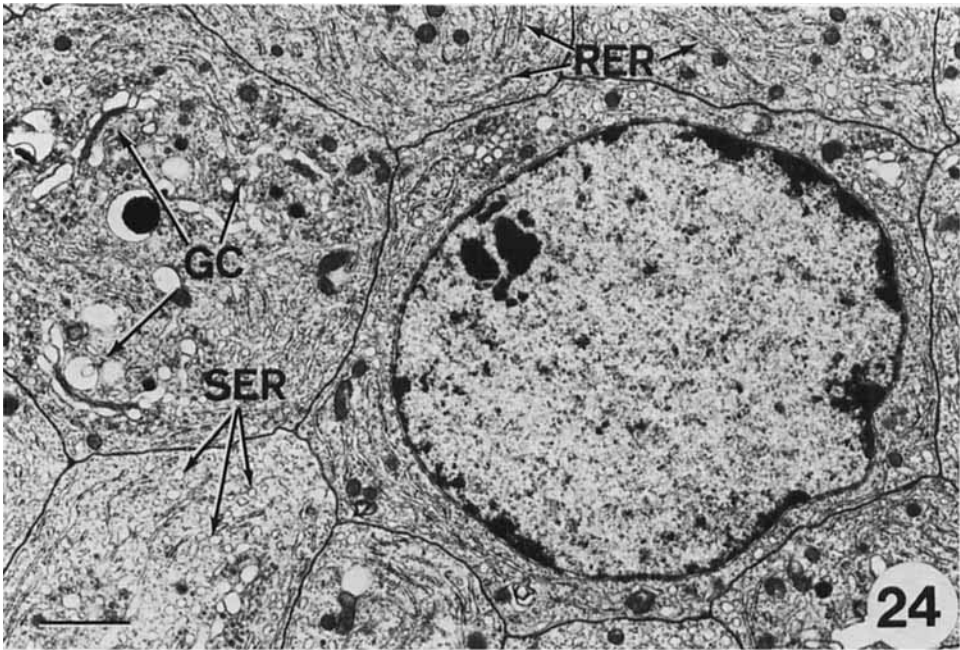
The spherical granules of cell type 2 show little modification as they pass toward the lumen. Similar granules are found in many

Fig. 24. Section near basal region of cell type 2. Cells possess several Golgi complexes (GC), abundant RER, and few simple granules. Vesicles of smooth endoplasmic reticulum (SER) are scattered throughout the cell cytoplasm. Bar = 1.0  $\mu$ m.

Fig. 25. Spherical granules and fused granules (arrows) at apical region of cell type 2. Fused granules result from the coalescence of spherical granules that have been released into small luminal pockets. Bar = 1.0  $\mu$ m.

Fig. 26. Golgi complex of cell type 1 showing cisternae, newly packaged secretory product (arrow), and mature granules. Most granules possess a clear space between the dense core and limiting membrane. Bar = 0.5  $\mu$ m.

Fig. 27. Paracrystalline granule showing consistent space of crystalline lattice. Bar = 0.1  $\mu$ m.



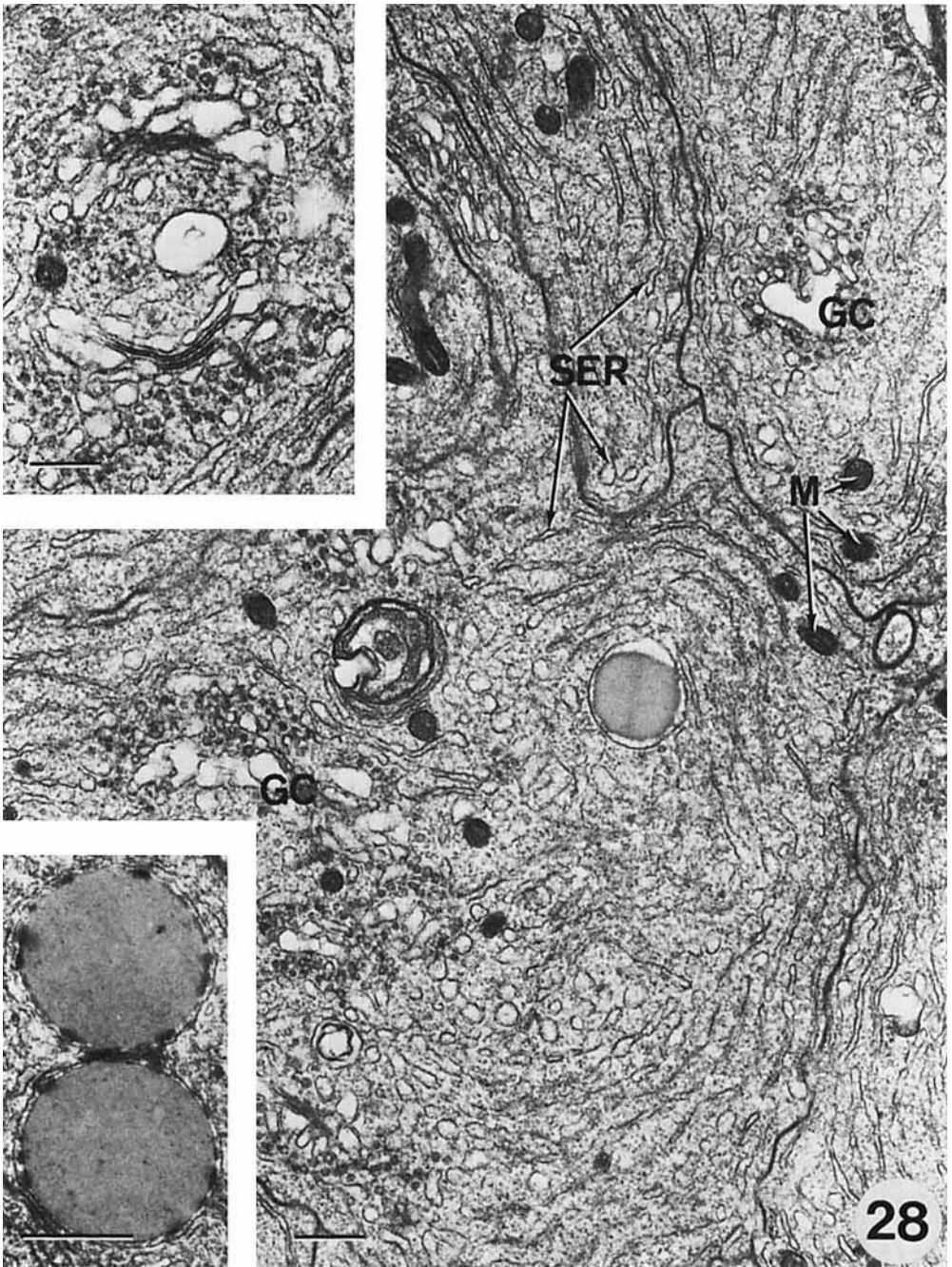


Fig. 28. Basal region of cell type 3 demonstrating numerous Golgi complexes (GC), several mitochondria (M), and abundant smooth endoplasmic reticulum (SER). Very few granules are present in this region of the cell. Inset at lower left illustrates deposition of wall material in lucent space between limiting membrane and granule matrix. Inset at upper left demonstrates several layers of Golgi cisternae. Bar = 0.5  $\mu$ m.

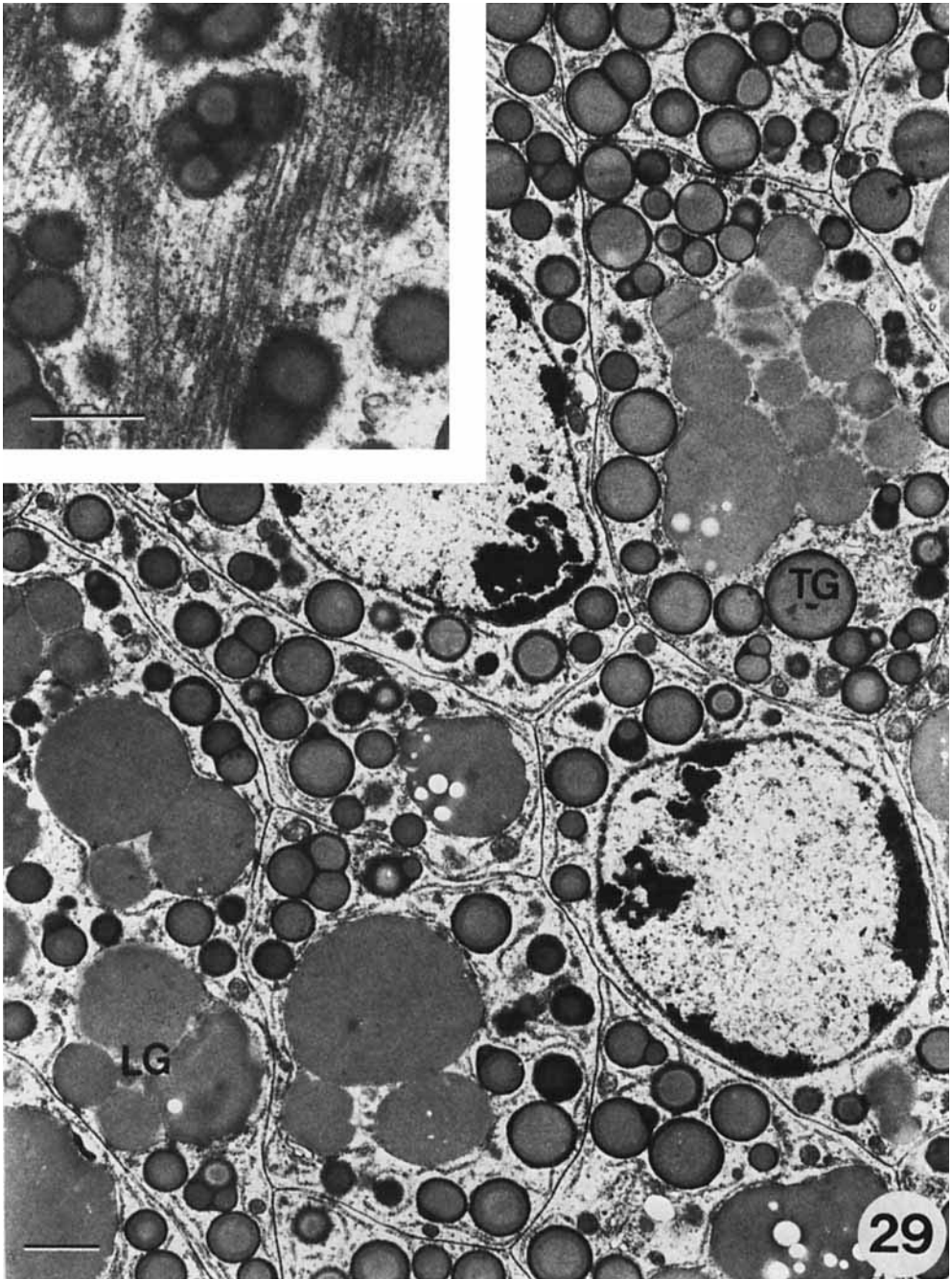
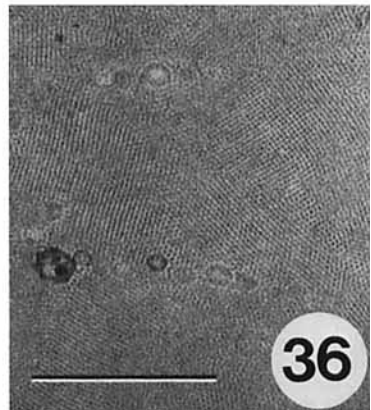
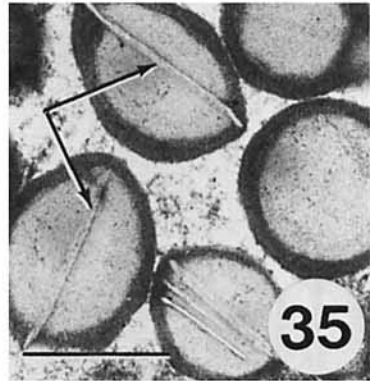
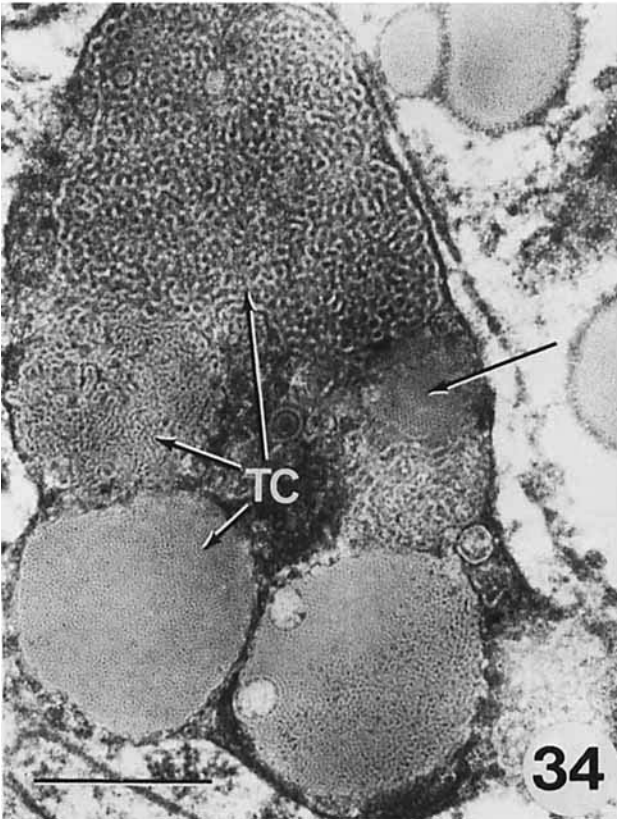
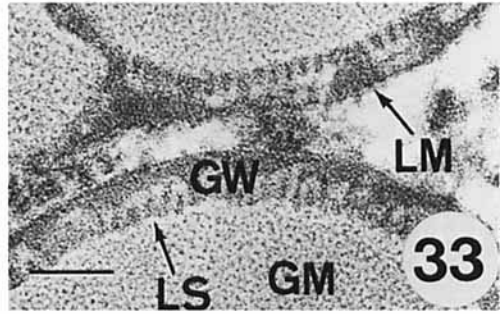
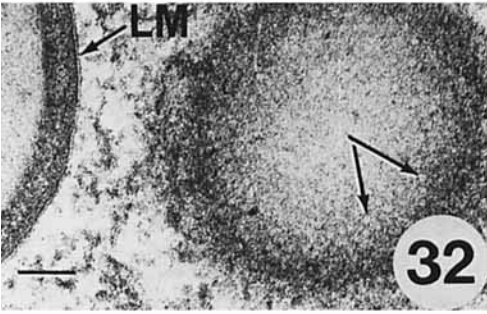
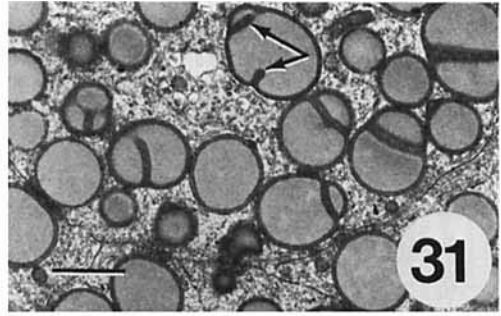
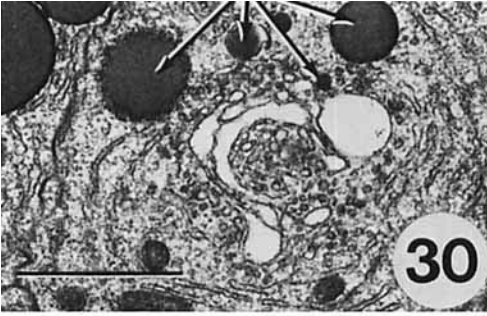


Fig. 29. Transverse section through mid-region of cell type 3. Notice thick-walled (TG) and lacework granules (LG) in cell cytoplasm. Bar = 1.0  $\mu\text{m}$ . Inset demonstrates microtubules traversing cell boundaries near the cell apex. Bar = 0.5  $\mu\text{m}$ .



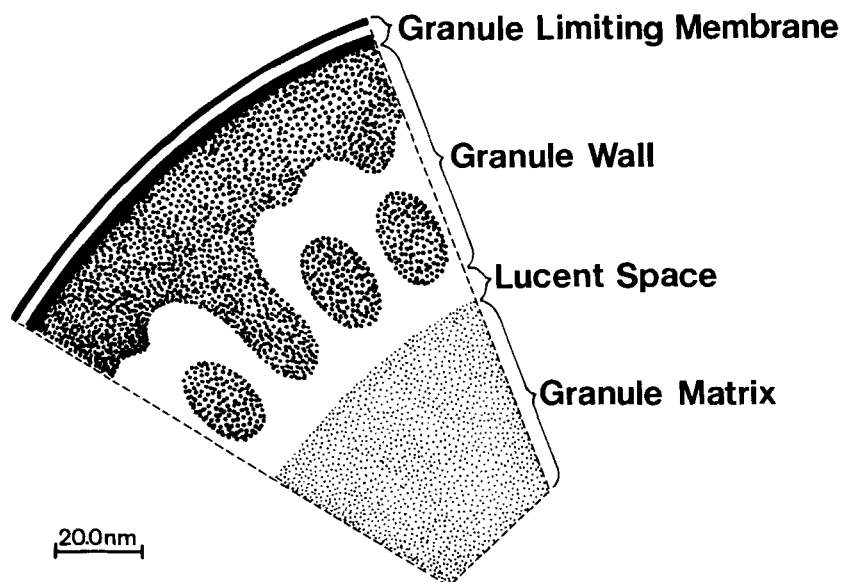


Fig. 37. Illustration of complex granule wall observed in cell type 3 granules. Region of wall near granule limiting membrane appears fairly homogeneous in most sections, while inner region of granule wall bordering granule matrix is sometimes variable in structure. Spaces between oval-shaped zones probably represent spherical elements observed in thin sections of this region (see Fig. 32). Bar = 0.02  $\mu\text{m}$ .

Fig. 30. Golgi complex in mid-region of cell type 3 appearing to elaborate simple granules (arrows). Note apparent increase in granule size during granule maturation. Bar = 1.0  $\mu\text{m}$ .

Fig. 31. Several granules in this micrograph are in the process of forming bilobed and multilobed granules through invagination of the granule wall and limiting membrane (arrows). Bar = 1.0  $\mu\text{m}$ .

Fig. 32. Section through the granule wall of a cell type 3 granule demonstrating the vesiculate appearance of the wall matrix (arrows). Portion of granule at left has definite limiting membrane (LM) above granule wall. Bar = 0.1  $\mu\text{m}$ .

Fig. 33. Micrograph showing complex structure of cell type 3 granules. For clarification, see Figure 37. Limiting membrane (LM), granule wall (GW), lucent space (LS), granule matrix (GM). Bar = 0.1  $\mu\text{m}$ .

Fig. 34. Large lacework granule of cell type 3 demonstrating inclusion spheres of varying substructure. Note different sizes of tubular convolutions (TC) and paracrystalline inclusion (arrow). Bar = 0.5  $\mu\text{m}$ .

Fig. 35. Rod-bearing granules of cell type 3. When rods are present (arrows) they tend to alter granule shape from spherical to ellipsoidal, with rod occupying long axis. Bar = 0.5  $\mu\text{m}$ .

Fig. 36. High-magnification view of paracrystalline inclusion observed in cell type 3. Note variation in crystalline orientation. Bar = 0.5  $\mu\text{m}$ .

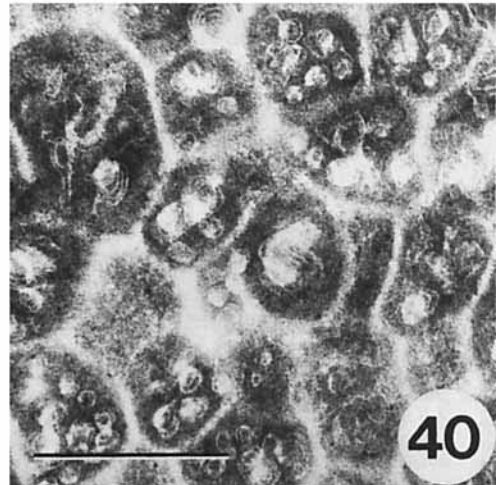
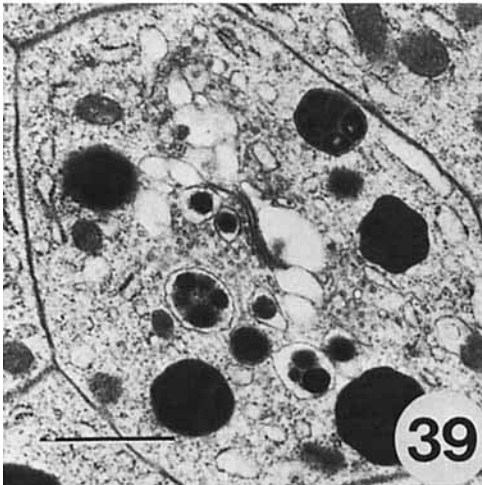
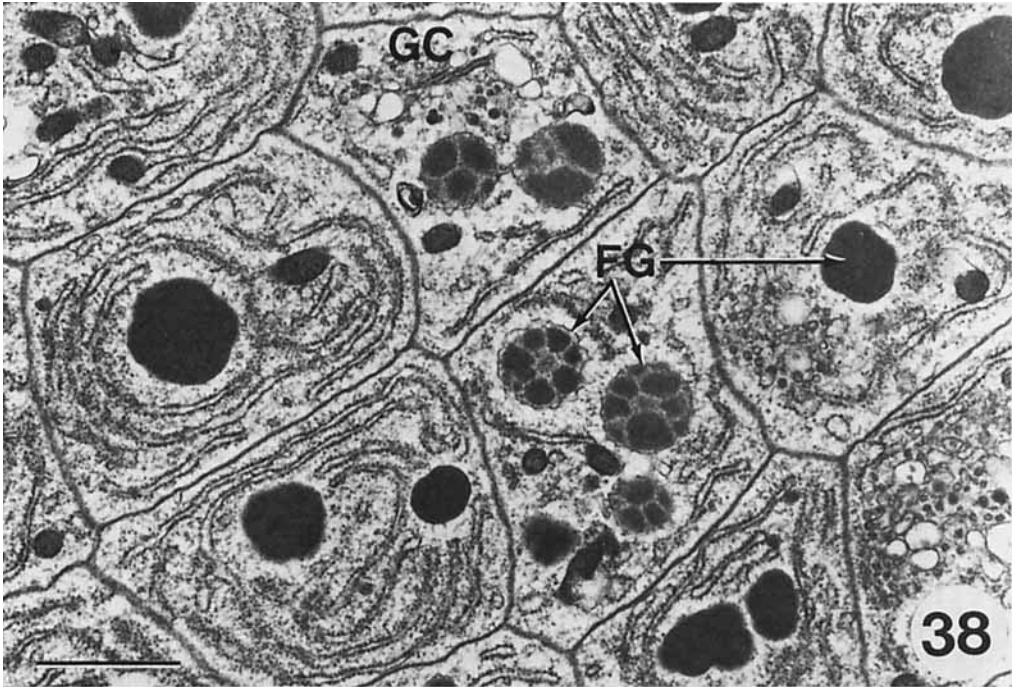


Fig. 38. Section through basal region of cell type 4. Characteristic rough endoplasmic reticulum (RER), Golgi complexes (GC), and faceted granules (FG) of various forms are observed. Bar = 1.0  $\mu$ m.

Fig. 39. Golgi complex in cytoplasm of cell type 4 with forming granules. Note how granules appear to begin as simple structures that eventually accumulate dense spheres. Bar = 1.0  $\mu$ m.

Fig. 40. Portion of secretory plug containing the unusual form of faceted granules described in the previous figures. Note that membrane fragments are still apparent in granules after elimination from the cell. Bar = 0.5  $\mu$ m.

Fig. 41. Oblique section through basal region of cell type 5. Granules appear electron-dense. Golgi complexes (GC) and RER predominate in this region. Bar = 1.0  $\mu$ m.

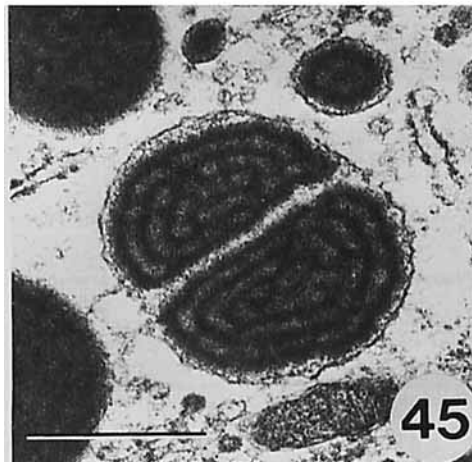
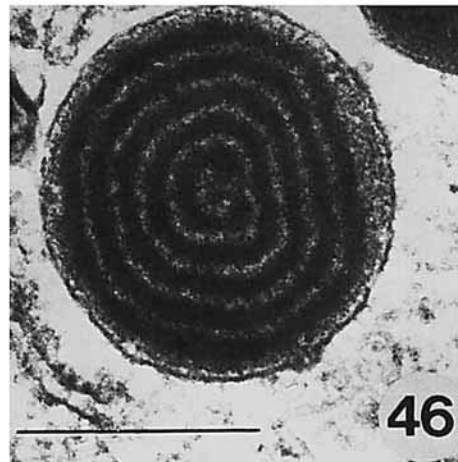
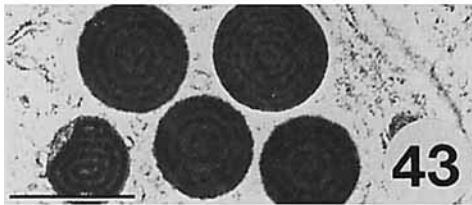
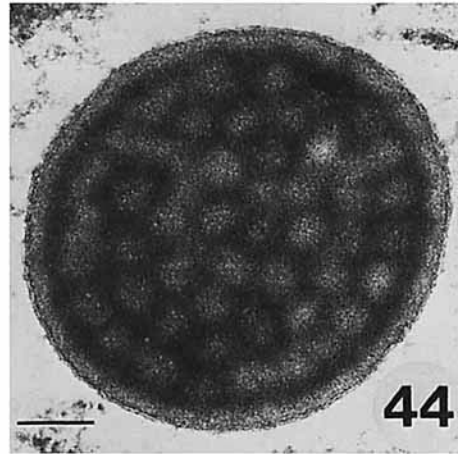
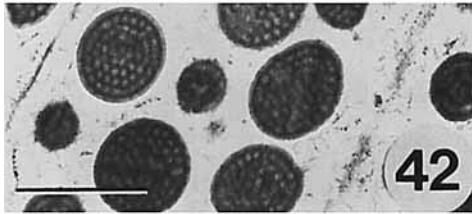
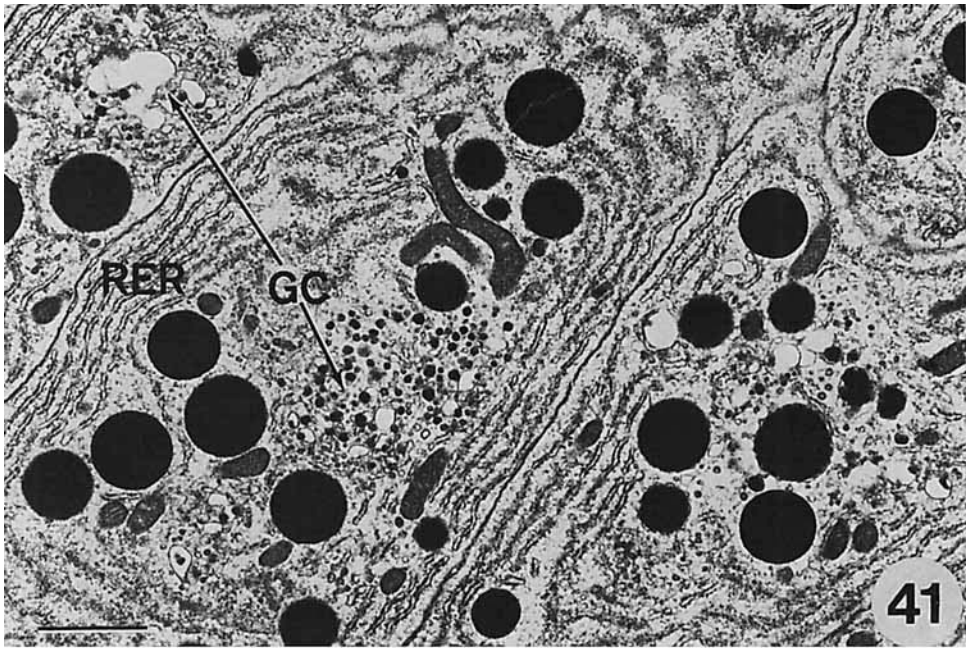
Fig. 42. Immature granules with many round electron-lucent spaces in the interior. Bar = 1.0  $\mu$ m.

Fig. 43. Mature concentric granules showing bull's-eye patterns and spirals. Bar = 1.0  $\mu$ m.

Fig. 44. Immature granule containing numerous round, lucent spaces of similar diameter. Note granule limiting membrane and absence of membranes in the granule matrix. Bar = 0.1  $\mu$ m.

Fig. 45. Bilobed concentric granule demonstrating patterns resulting from probable coalescence of round spaces on the granule matrix. Bar = 0.5  $\mu$ m.

Fig. 46. Bull's-eye pattern of concentric granule showing light and dark rings. Bar = 0.5  $\mu$ m.



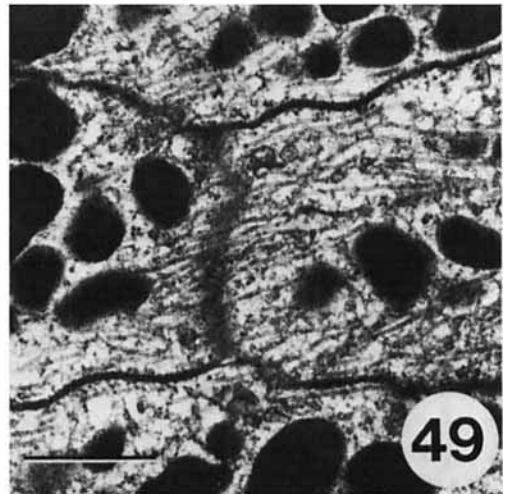
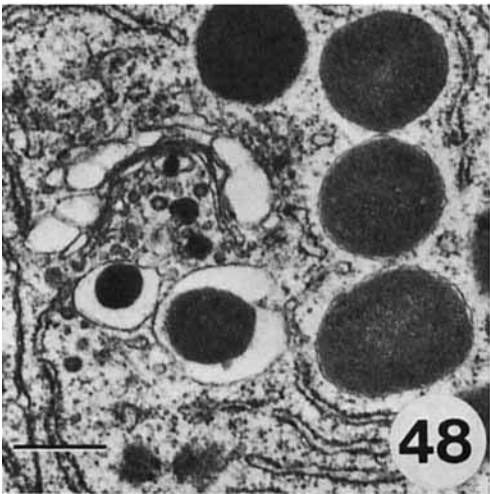
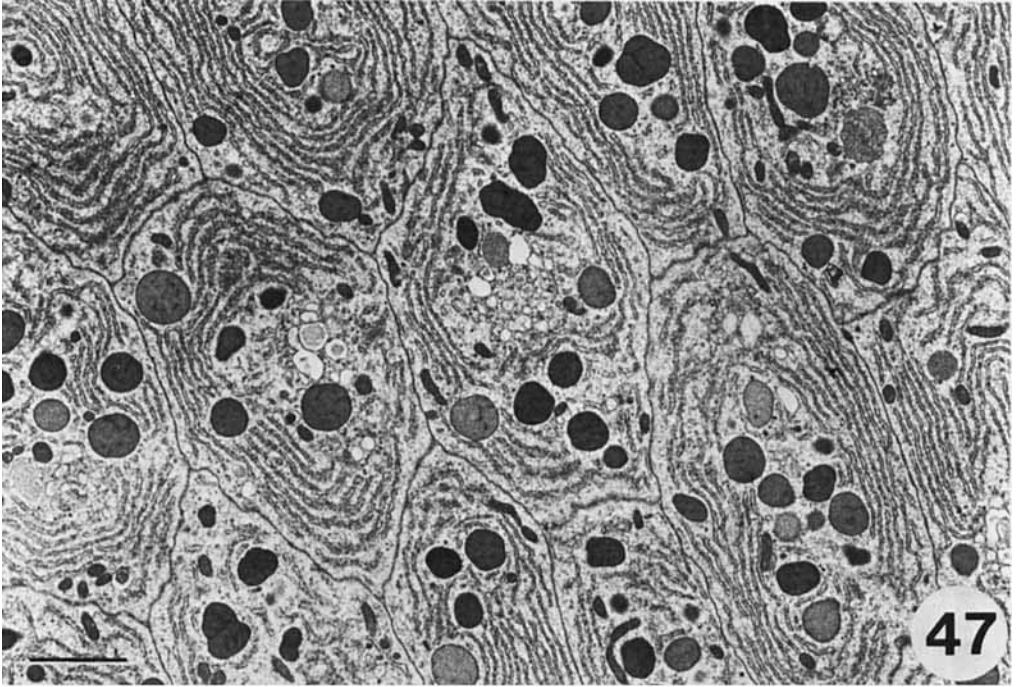


Fig. 47. Transverse section through basal region of cell type 6. Note abundance of RER and numerous Golgi complexes. Granules of varying electron density exist in the cytoplasm. Less electron-dense granules may represent immature forms. Bar =  $2.0 \mu\text{m}$ .

Fig. 48. Golgi complex of cell type 6 showing packaging of secretory product and various stages of development. Bar =  $0.5 \mu\text{m}$ .

Fig. 49. Apical region of type 6 cells showing several granules and numerous microtubules traversing the cell membranes. Bar =  $1.0 \mu\text{m}$ .

cells, including the beta cells of mouse pancreas (Slavin et al., '77), the azurophil cells of guinea pig heterophil granulocytes (Brederoo and Daems, '78), the yolk cells of a bryozoan (Terakado and Mukai, '78), and the follicle cells of a Colorado potato beetle (DeLoof, '71).

The granules of cell type 6 are only slightly modified from their formation near the Golgi (large core of moderate electron density and narrow halo) to the mature form (granular "shaded" contents that fill the space of the vesicle). Such granules are found in diverse tissues, including insect haemocytes (Brehélin et al., '76), lizard kidneys (Davis et al., '76), and rat atria (Theron et al., '78ab).

Two secretory cells, types 1 and 5, contain granules with an electron-dense homogenous grainy matrix within which lie spherical, electron-transparent spaces. In both types 1 and 5, the electron-transparent spaces fuse. In type 1 the result tends toward simple granules with a large (sometimes single), prominent clear core and a dense cortex. The clear spheres in type 5 granules are all of similar size, and as they fuse with one another, the result is spirals or concentric rings of dense material. Granules similar to those of type 1 are often associated with autophagocytic activity in insects (Simões et al., '77) or with vertebrate exocrine glands such as mouse prostate described by Franks and Barton ('60). The bull's-eye granules of type 5 cells are quite similar to the cortical granules of sea urchin eggs (Takashima, '60; Anderson, '68; Schuel et al., '69), which contain acidic mucopolysaccharides, and to granules of the salivary glands of primitive mammals (mandibular glands of *Echidna*; Lennep et al., '78) and submandibular glands of a hedgehog (Tandler and MacCallum, '72).

Shortly after they form, the secretory granules of type 4 cells are partitioned into angular, electron-dense zones in a less dense matrix. Similar granules are found in the male accessory glands of cockroaches (Ballan-Duffrancais, '70) and of dogs (Brandes, '74), and in the armadillo submandibular gland (Ruby and Canning, '78).

The most pleiomorphic granules are those of type 7 cells, which contain a great diversity of membranes, whorls, tubular arrays, etc. Similar myelin-like forms are found in ejaculatory ducts of flour moths (Riemann and Thorson, '79b), the epididymis of the rat (Brandes, '74), and the thoracic ganglia of a grasshopper (Lane, '68).

The thick-walled granules of cell type 3 are

unique in several respects: (1) They begin as single-compartment granules whose outer wall forms by condensation of dense plaques (Fig. 28); (2) they become subdivided by invagination of the organized wall; (3) the wall itself is most unusual. Although often secretory granules in many other tissues have distinct walls and medullae, none that we have encountered possess these characteristics. We assume that the strong affinity of type 3 cells for Oil Red O is due to the partitioning of this dye into type 3 secretory granules.

It would be useful to relate the morphology of the secretory granules to the chemical composition of the products, but our preliminary histochemical data is only suggestive, and we have not yet achieved separation of the various types of granules from one another. At present we can only emphasize that most of the secretory cells (except perhaps for type 3, with its abundant smooth endoplasmic reticulum) export granules that contain significant amounts of protein. In any case, the characteristic morphology of the various granules allows precise mapping of the secretory cell types in the epithelium and of the products of each cell in the secretory plug.

#### *Organized layers in the secretory product*

Insect secretory systems produce many solid, organized structures. Among these are the basement membranes, the food webs of blackflies, the silk, the cuticle, the chorion, the peritrophic membrane, and the spermatophore.

The basement membrane is relatively simple in its structure and mode of formation. It is similar in fine structure throughout its thickness, and apparently it is formed by successive apposition of materials discharged by blood cells (Wigglesworth, '79). The food web of midges (*Chironomus*) contains several structural proteins, is secreted rapidly and renewed by periodic episodes, and is like the basement membrane in being structurally homogenous rather than layered (references in Grossbach, '77). The most specialized biosynthetic parsimony is found in some silk glands, which secrete mostly fibroin (70–80%) and sericin (20–30%) (Suzuki, '77). In all three cases, the product is homogenous rather than being distributed in distinct layers.

In the cuticle, the chorion, the peritrophic membrane, and the spermatophore, the macromolecules exported by secretory cells are variously localized in discrete layers within

the secretory product. Layered structures are formed by two mechanisms: (1) serial export of successive product from a single cell type (cuticle, chorion), or (2) parallel export of dissimilar products by diverse cell types (peritrophic membrane, spermatophore).

Serial export for the formation of insect cuticle has been extensively studied (see Locke, '74; Neville, '75; Hepburn, '76). A succession of layers is formed containing varying amounts of lipid within the subcuticular space, beginning with the outermost layer (epicuticular) and proceeding to the innermost layer (procuticular). In addition, some materials are inserted within the previously formed layers by intussusception (e.g., Condoulis and Locke, '66). The serial synthesis and export of these components is carried out mostly by the epidermal cell, whose synthetic program is controlled by circulating ecdysteroids, juvenile hormones, and other factors (Gilbert and King, '73). Molecular dissection of the secretory phenomenology within these epidermal cells has been complicated by the complexity and insolubility of the product as well as by rapid transition from one phase of the secretory program to the next.

Chorion proteins are more easily solubilized than cuticular proteins (Kawasaki et al., '71), and secretion of the chorion by follicular cells in *Drosophila* and silkmoths has proved more susceptible to molecular analyses than has cuticular production (Kafatos et al., '77; Spradling and Mahowald, '79; Waring and Mahowald, '79). The chorion is laid down by a succession of programmed syntheses and exports, as is cuticle. At least in the silkmoth, the initial protein secretion establishes a framework, and then other export proteins are added either by intussusception or by apposition on the surface near the secretory follicular cells (Blau and Kafatos, '79). The follicular cells differ from many other secretory systems in that they act only once to produce and export product, after which these cells degenerate.

The peritrophic membrane of the gut of many insects is concerned with protection of midgut cells from abrasion as well as other digestive roles. Its components include both chitin and protein (Waterhouse, '57; Wigglesworth, '72). In the blowfly this membrane is laid down by several distinct cell types, which secrete in parallel (Smith, '68). Biochemical analyses of the formation of the peritrophic membrane are complicated by contamination of the preparations with other insect proteins (digestive enzymes, etc.) as well as exogenous materials introduced in the food.

Like the peritrophic membrane, spermatophores are formed by the combination of the secretory products of several distinct cell types that export in parallel with each other. In the orthopteroid insect, the long male accessory glands responsible for the spermatophore production are usually divided into many tubules of varying lengths (Davey, '65; Wigglesworth, '72). The product of these tubules are histologically and histochemically distinct (*Locusta*—Cantacuzène, '67; Gregory, '65a, b; *Gomphocerus*—Hartmann, '70; *Schistocerca*—Cantacuzène, '67; Odhiambo, '69; *Blattella*—Khalifa, '50a; Ballan-Dufrançais, '68). In *Acheta*, Kaulenas ('76) has shown that the contents of electrophoretically displayed proteins and the amino acid incorporation profiles differ among the various tubes. The fluid products of each of the glands flow into the ejaculatory duct and coalesce and harden during transport through that duct and into the female bursa (e.g., Hohorst, '36). Similar secretory phenomena have been found in *Rhodnius*, a bug (Davey, '59), and in moths (*Heliothis*—Callahan and Cascio, '63; *Galleria*—Khalifa, '50b; *Anagasta*—Riemann and Thorson, '79ab).

In many beetles, several cell types are found in each accessory gland. The primary glandular product is an elastic, sticky solid mass, which we have termed the secretory plug. The plug is organized into layers in the meloid (*Lytta*—Gerber, '68; Gerber et al., '71ab), in a

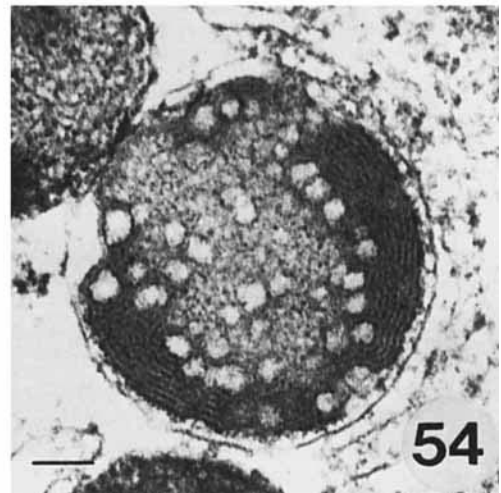
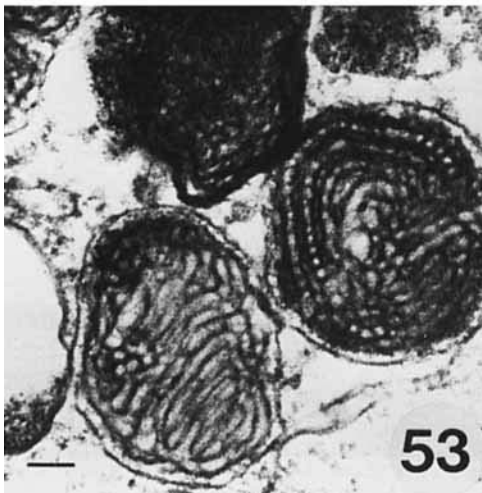
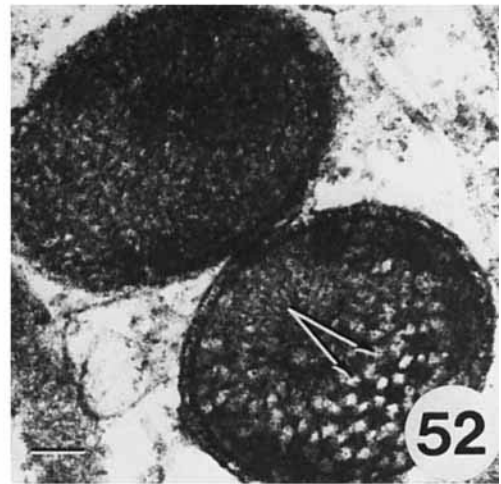
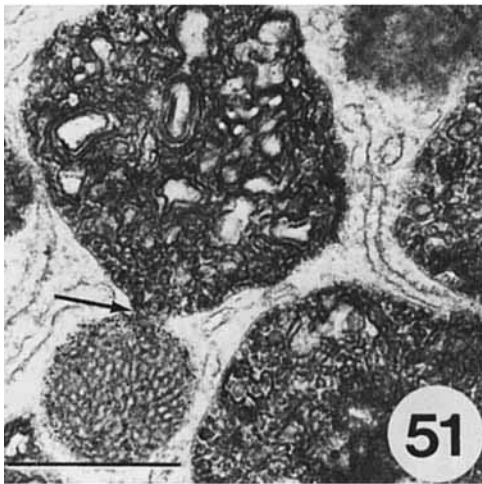
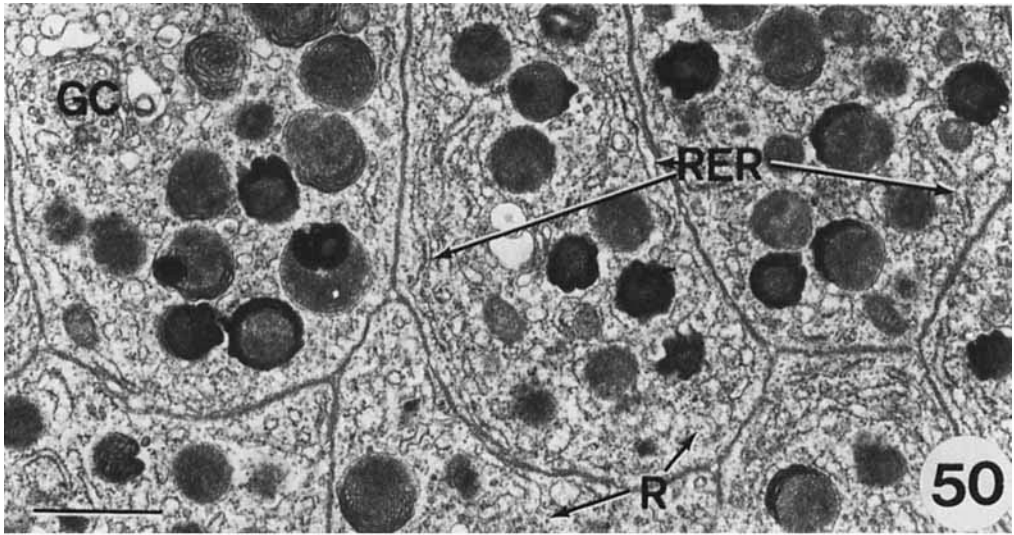
Fig. 50. Basal region of cell type 7 with secretory granules, RER, free ribosomes (R), Golgi complexes (GC), and mitochondria occupying the cell cytoplasm. Bar = 1.0  $\mu$ m.

Fig. 51. Complex granule with characteristic meshwork of tubules and membranes. Note connection between granules (arrow). Bar = 0.5  $\mu$ m.

Fig. 52. Secretion granule with pentaradiate pattern of dense elements (arrows). Bar = 0.1  $\mu$ m.

Fig. 53. Varied patterns of membrane profiles. Bar = 0.1  $\mu$ m.

Fig. 54. Granule containing stacked membranes near the periphery and scattered clear zones in the granule matrix. Bar = 0.1  $\mu$ m.



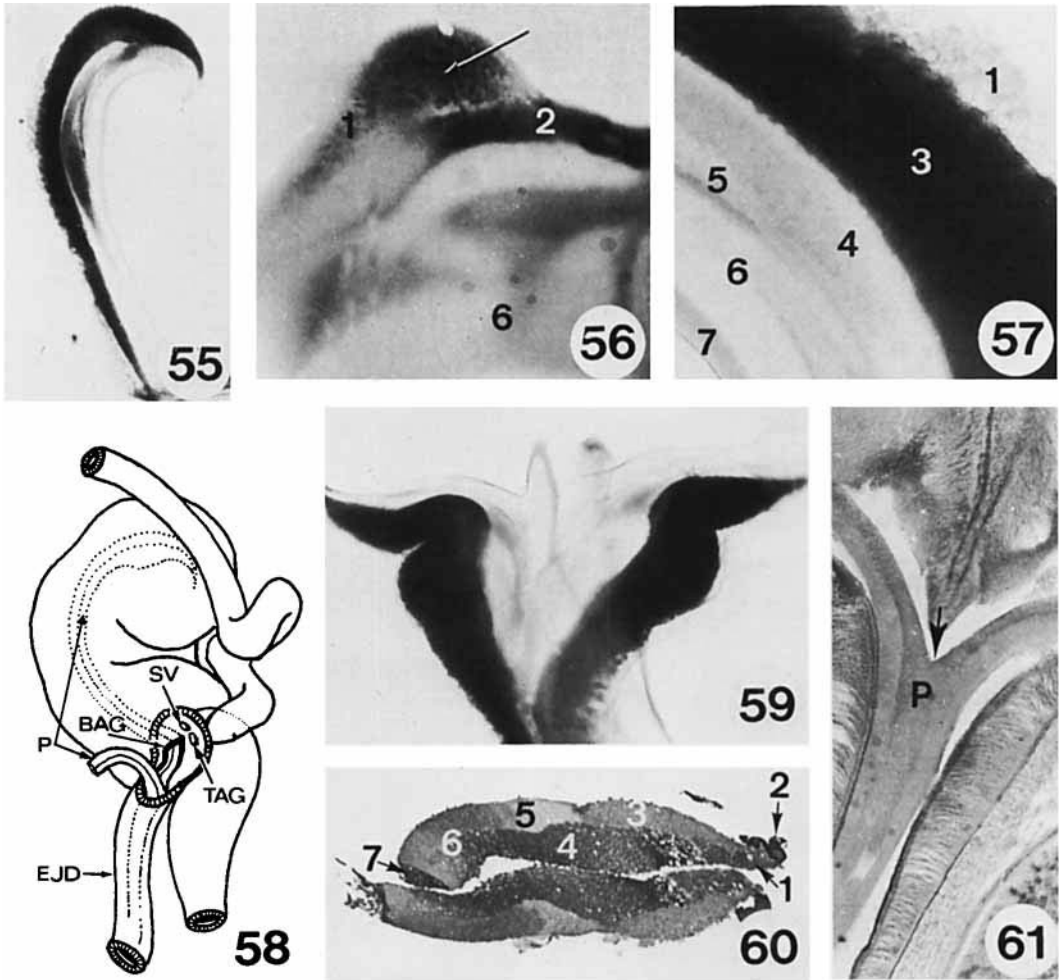


Fig. 55. Plug removed from BAG after staining with Oil Red O.  $\times 51$ .

Fig. 56. Elevated portion of plug (arrow) indicates region where secretions of cell types 1 and 2 mix with one another. Although the secretory products mix, there is no fusion or blending of individual granule types into a homogeneous mixture. Whole mount, trypan blue.  $\times 238$ .

Fig. 57. Portion of plug showing zones formed by secretory granules of BAG secretory cells. Oil Red O.  $\times 297$ .

Fig. 58. Illustration showing inside lateral view of the grand junction. It is at this junction that the secretory products of the accessory glands (BAG, TAG) and seminal vesicles (SV) empty into the ejaculatory duct (EJD). P, plug; BAG, bean-shaped accessory gland; SV, seminal vesicle; TAG, tubular accessory gland; EJD, ejaculatory duct.  $\times 19$ .

Fig. 59. View of the distal portion of individual BAG plugs prior to complete fusion. Notice how plug zones fuse with mirror-image counterparts. Oil Red O.  $\times 107$ .

Fig. 60. EM thick section of BAG plugs lying side by side prior to entering the ejaculatory duct. Numbers correspond to secretory product secreted by BAG cell types. Toluidine blue.  $\times 265$ .

Fig. 61. Longitudinal section showing junction of secretory plugs and their point of fusion in the bifurcated ejaculatory duct. Bouin's, paraffin, PAS.  $\times 51$ .

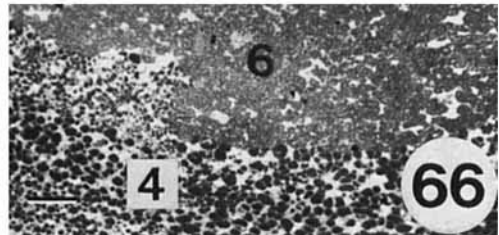
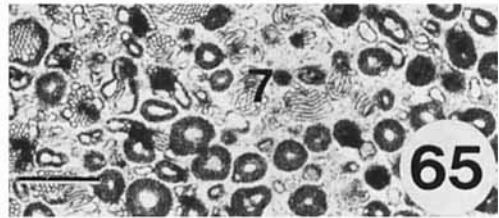
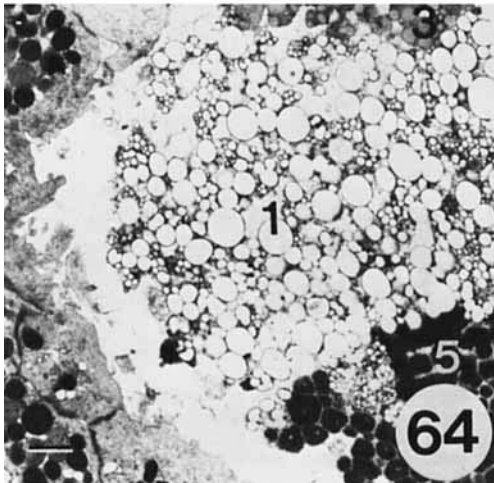
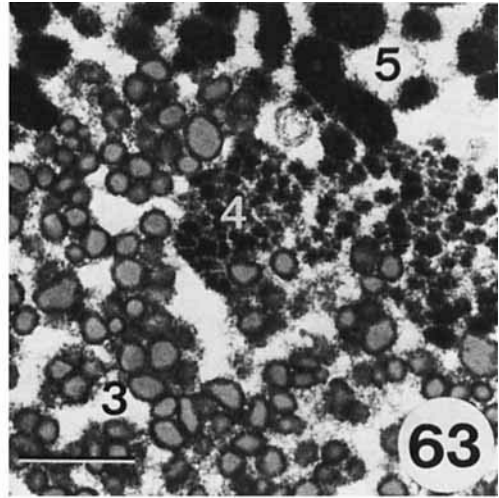
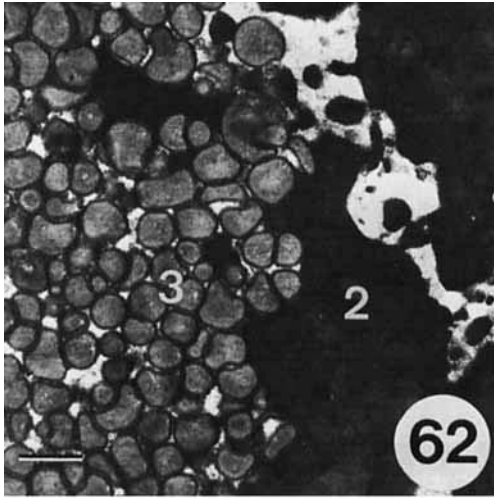


Fig. 62. Region of plug where secretion products of cell type 2 and 3 occur. Bar = 1.0  $\mu$ m.

Fig. 63. Portion of plug from which three separate secretory products can be identified. Lower left, cell type 3 granules; middle, cell type 4; top, cell type 5 granules. Bar = 1.0  $\mu$ m.

Fig. 64. Portion of plug containing secretory products of cell types 1, 3, and 5. Bar = 1.0  $\mu$ m.

Fig. 65. Cell type 7 secretion as it appears in plug. Bar = 1.0  $\mu$ m.

Fig. 66. Regions of plug containing secretory products of cell type 4 and cell type 6. Bar = 2.0  $\mu$ m.

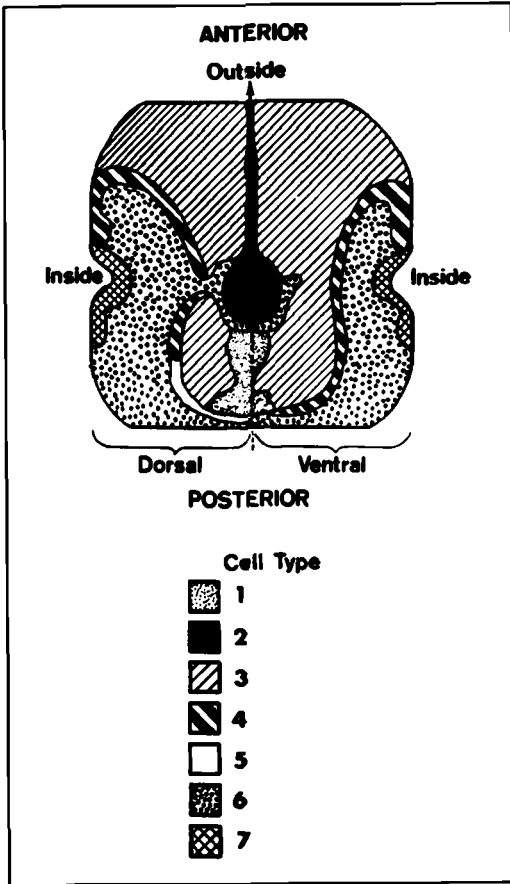


Fig. 67. Eckart projection of bean-shaped accessory gland illustrating relative area, abundance, and symmetry of cell types. Folding the gland in half by way of the outside lateral dashed line yields a generalized view of dorsal and ventral surfaces, as illustrated in Figure 3.  $\times 14$ .

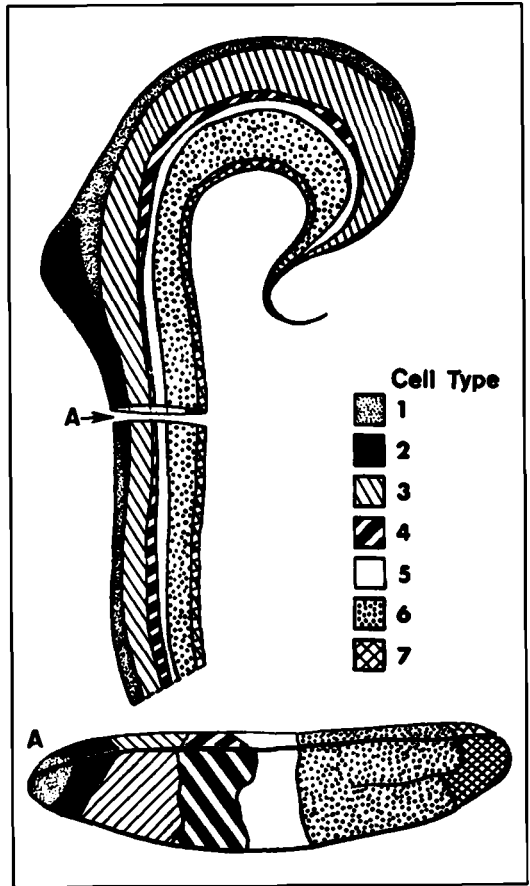


Fig. 68. Plug produced by secretions of the seven cell types composing the bean-shaped accessory gland. Transverse slice (A) illustrates typical zonation of secretory product as observed in thin section. Plug (P),  $\times 85$ ; section A,  $\times 130$ .

bruchid (*Acanthosceldes*—Huignard, '75), in an elaterid (*Ctenicera*—Zacharuk, '58), and in tenebrionids (*Pimelia*—Fiori, '54; *Tenebrio*—Gadzama, '71; Gerber, '76; this report). The plug is not a random mixture of cell secretions, but it is invariably organized into zones that differ in their staining characteristics and in their chemical composition. In order for a proper plug to form, each population of cells of each type must export in concert an appropriate quantity of product, and all the cell types must export in a coordinated, balanced manner.

Upon mating, the plug exits the gland and enters the ejaculatory duct in *Lytta* (Gerber et

al., '71b), in *Ctenicera* (Zacharuk, '58), in *Acanthosceldes* (Huignard, '75), and in *Tenebrio* (this study). The accessory glands must then rapidly secrete a new plug (Gerber et al., '71b; Huignard, '75; this study). Since these beetles mate several times, the gland can be "milked" repeatedly. In *Tenebrio* the proteins are easily solubilized and displayed on SDS gels. The relative protein content within spermatophore masks is constant over repeated milkings (up to seven for *Tenebrio* as demonstrated in our laboratory). Thus, the mechanisms of recurrent secretory episodes can be conveniently studied.

In both *Tenebrio* and *Lytta* the layers of the

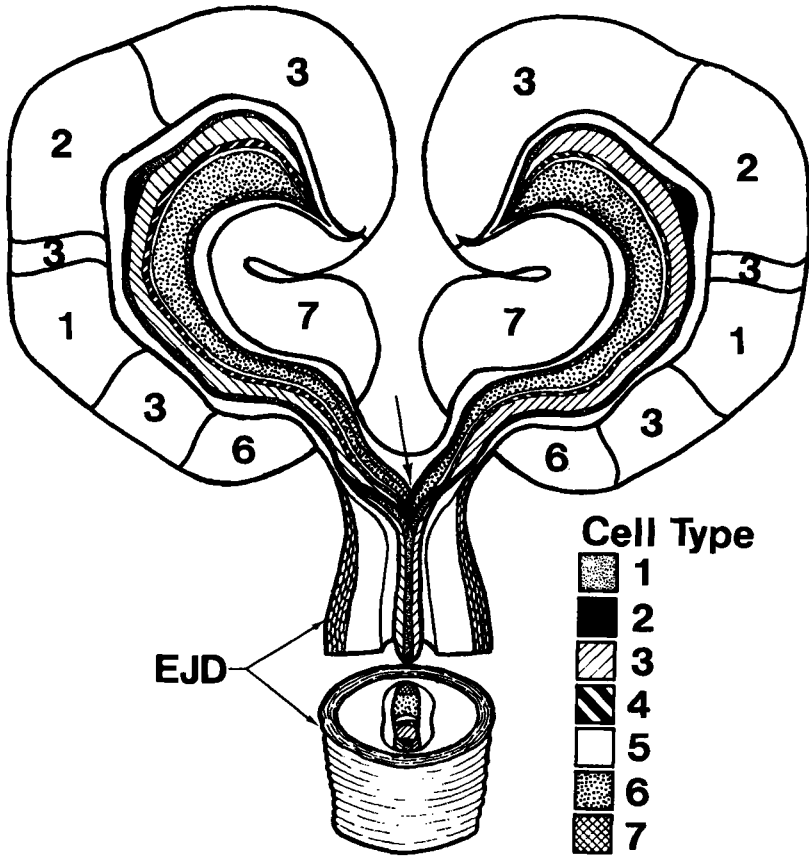


Fig. 69. Schematic diagram of BAG plugs entering ejaculatory duct (EJD) and fusing to form a single structure. Glands are represented in medio-frontal section. Note: Since this is only one plane of section, the regions occupied by cell types 4 and 5 in the gland are not shown, but their secretory products are shown in the secretory plug. Arrow indicates place where plugs fuse.  $\times 29$ .

plugs are not arranged in the same order as are the homologous layers of the spermatophore wall. In *Lytta*, Gerber et al. ('71b) have described quite nicely the flowing of the layers across one another as the spermatophore is formed. We do not yet have such a detailed description for *Tenebrio*. In *Tenebrio*, the two secretory plugs fuse at the origin of the ejaculatory duct and become more elastic as the mass flows rearward and the constituent layers are rearranged. The result, an organized spermatophore, has an infolded tip and three coils when it is ejected from the intromittent organ (Gadzama and Happ, '74).

The coordinated parallel secretory episodes in the several cell types, the nature and number of secretory products, the transformation of the solid plug into a spermatophore, and the differentiation of the glands responsible will be the subjects of future papers in this series.

ACKNOWLEDGEMENTS

We are grateful for support from the National Institutes of Health (NIAMD 15662 and NIGMS 26140). We thank Bonnie J. MacLeod for technical assistance and Joyce Murray for typing the manuscript.

## LITERATURE CITED

- Abraham, R. (1934) Das Verhalten der Spermien in der weiblichen Bettwanze (*Cimex lectularis*) und der Verbleib der überschüssigen Spermamasse. *Z. Parasitk.*, 6:559-591.
- Anderson, E. (1968) Oocyte differentiation in the sea urchin, *Arbacia punctulata*, with particular reference to the origin of cortical granules and their participation in the cortical reaction. *J. Cell Biol.*, 37:514-539.
- Baccetti, B. (1972) Insect sperm cells. In: *Advances in Insect Physiology*. V. J.M. Treherne, M.J. Berridge, and V.B. Wigglesworth, eds. Academic Press New York, pp. 316-397.
- Ballan-Dufrançais, C. (1968) Données morphologiques et histologiques sur les glandes annexes mâles et le spermatophore de *Blattella germanica* au cours de la vie imaginaire. *Bull. Soc. Zool. France*, 93:401-421.
- Ballan-Dufrançais, C. (1970) Données cytophysiologiques sur un organe excréteur particulier d'un insecte, *Blattella germanica* L. (Dictyoptera). *Z. Zellforsch.*, 109:336-355.
- Baumann, H. (1974) Biological effects of paragonial substances PS-1 and PS-2 in females of *Drosophila funebris*. *J. Insect Physiol.*, 20:2347-2362.
- Bishop, G.H. (1920) Fertilization in the honey-bee I. The male sexual organs: their histological structure and physiological functioning. *J. Exp. Zool.*, 31:225-259.
- Blau, H.M., and F.C. Kafatos (1979) Morphogenesis of the silkworm chorion. *Dev. Biol.*, 72:211-225.
- Bouletreau, J. (1974) Importance relative des stimulations de l'accouplement: parade, copulation et insémination sur la production ovarienne de *Drosophila melanogaster*. *Bull. Biol. Fr. Belg.*, 108:61-70.
- Brandes, D. (1974) Fine structure and cytochemistry of male sex accessory organs. In: *Male Accessory Sex Organs*. D. Brandes, ed. Academic Press, New York: pp. 18-113.
- Brederoo, P., and W. Th. Daems (1978) The ultrastructure of guinea pig heterophil granulocytes and the heterogeneity of the granules. *Cell Tissue Res.*, 194:183-205.
- Brehélin, M., D. Zachary, and J.A. Hoffman (1976) Fonctions des granulocytes typiques dans la cicatrisation chez l'orthoptère *Locusta migratoria* L. *J. Microsc. Biol. Cell.*, 25:133-136.
- Callahan, P.S., and T. Cascio (1963) Histology of the reproductive tracts and transmission of sperm in the corn earworm, *Heliothis zea*. *Ann. Entomol. Soc. Am.*, 56:535-556.
- Cantacuzène, A.M. (1967) Recherches morphologiques et physiologiques sur les glandes annexes mâles des orthoptères. I. Histophysiologie de l'appareil glandulaire des acridiens, *Schistocerca gregaria* et *Locusta migratoria*. *Bull. Soc. Zool. France*, 92:725-738.
- Condoulis, W.V., and M. Locke (1966) The deposition of endocuticle in an insect *Calpodus ethlius* Stoll (Lepidoptera, Hesperidae). *J. Insect Physiol.*, 12:311-323.
- Crick, F.H.C., and P.A. Lawrence (1975) Compartments and polyclones in insect development. *Science*, 189:340-346.
- Davey, K.G. (1959) Spermatophore production in *Rhodnius prolixus*. *Quart. J. Microsc. Sci.*, 100:221-230.
- Davey, K.G. (1960) The evolution of the spermatophore in insects. *Pro. R. Entomol. Soc. London, Ser. A*, 35:107-113.
- Davey, K.G. (1965) *Reproduction in the Insects*. W.H. Freeman. San Francisco.
- Davis, L.E., B. Schmidt-Nielsen, and H. Stolte (1976) Anatomy and ultrastructure of the excretory system of the lizard, *Sceloporus cyanogenys*. *J. Morphol.*, 149:279-326.
- DeLoof, A. (1971) Synthesis and deposition of oocyte envelopes in the Colorado beetle, *Leptinotarsa decemlineata* Say. *Z. Zellforsch.*, 115:351-360.
- Dulbecco, R., and M. Vogt (1954) Plaque formation and isolation of pure lines with poliomyelitis viruses. *J. Exp. Med.*, 99:167-182.
- Encyclopedia Britannica World Atlas (1945) C.S. Hammond Co., New York.
- Fiori, G. (1954) Morfologia addominale, anatomia ed histologia degli apparati genitali de "*Pimelia angulata confalonieri*." Grid. (Coleoptera: Tenebrionidae) formazione dello spermatoforo. *Boll. Ist. Entomol. Univ. Bologna*, 20:377-422.
- Franks, L.M., and A.A. Barton (1960) The effects of testosterone on the ultrastructure of the mouse prostate *in vivo* and in organ cultures. *Exp. Cell Res.*, 19:35-50.
- Frenk, E., and G.M. Happ (1976) Spermatophore of the mealworm beetle: Immunohistochemical characteristics suggest affinities with male accessory gland. *J. Insect Physiol.*, 22:891-895.
- Gadzama, N.M. (1971) A histological, histochemical, and electron microscopical study of the spermatophore and the internal reproductive organs of male *Tenebrio molitor* L. (Coleoptera: Tenebrionidae). Ph.D. Thesis, New York University.
- Gadzama, N.M., and G.M. Happ (1974) The structure and evacuation of the spermatophore of *Tenebrio molitor* L. (Coleoptera: Tenebrionidae). *Tissue Cell*, 6:95-108.
- Gadzama, N.M., C.M. Happ, and G.M. Happ (1977) Cyto-differentiation in the accessory glands of *Tenebrio molitor*. I. Ultrastructure of the tubular gland in the post-ecdysial adult male. *J. Exp. Zool.*, 200:211-222.
- Gerber, G.H. (1968) Structure, formation, histochemistry, fate and functions of the spermatophore of the Caragana blister beetle, *Lytta nuttalli* Say (Coleoptera: Meloidae). Ph.D. Thesis, University of Saskatchewan, Saskatoon.
- Gerber, G.H. (1976) Reproductive behavior and physiology of *Tenebrio molitor* (Coleoptera: Tenebrionidae) III. Histogenetic changes in the internal genitalia, mesenteron, and cuticle during sexual maturation. *Can. J. Zool.*, 54:990-1002.
- Gerber, G.H., N.S. Church, and J.G. Rempel (1971a) The anatomy, histology, and physiology of the reproductive systems of *Lytta nuttalli* Say (Coleoptera: Meloidae) I. The internal genitalia. *Can. J. Zool.*, 49:523-533.
- Gerber, G.H., N.S. Church, and J.G. Rempel (1971b) The structure, formation, histochemistry, fate, and functions of the spermatophore of *Lytta nuttalli* Say (Coleoptera: Meloidae). *Can. J. Zool.*, 49:1595-1610.
- Gilbert, L.I., and D.S. King (1973) Physiology of growth and development: endocrine aspects. In: *The Physiology of Insecta*. M. Rockstein, ed. Academic Press, New York, pp. 249-370.
- Gillett, J.D. (1958) Induced ovarian development in decapitated mosquitoes by transfusion of haemolymph. *J. Exp. Biol.*, 35:684-693.
- Gregory, G.E. (1965a) On the initiation of spermatophore formation in the African migratory locust, *Locusta migratoria migratorioides* Reiche and Fairmaire. *J. Exp. Biol.*, 42:423-435.
- Gregory, G.E. (1965b) The formation and fate of the spermatophore in the African migratory locust, *Locusta migratoria migratorioides* Reiche and Fairmaire. *Tans. R. Entomol. Soc. Lond.* 117:33-66.
- Grimes, M.I., and G.M. Happ (1980) Cytodifferentiation in the accessory glands of *Tenebrio molitor*. V. Fine structure of the bean-shaped gland in the male pupa. *Int. J. Insect Morphol. Embryol.* (in press).
- Grossbach, V. (1977) The salivary gland of *Chironomus* (Diptera): a model system for the study of cell differentiation. In: *Results and Problems in Cell Differentiation*, Vol. 8. Biochemical Differentiation in Insect Glands. Springer-Verlag, Berlin, Heidelberg, New York, pp. 1-44.
- Happ, G.M., C. Yunker, and S.A. Huffmire (1977) Cytodifferentiation in the accessory glands of *Tenebrio molitor*. II. Patterns of leucine incorporation in the tubular glands of post-ecdysial adult males. *J. Exp. Zool.*, 200:223-236.

- Hartmann, R. (1970) Experimentelle und histologische Untersuchungen der Spermatophorenbildung bei der Feldheuschrecke *Gomphocerus rufus* L. (Orthoptera, Acrididae). *Z. Morphol. Tiere*, **68**:140-176
- Hepburn, H.R. (1976) *The Insect Integument*. Elsevier-North Holland, New York.
- Hinton, H.E. (1964) Sperm transfer in insects and the evolution of haemocoelic insemination. *R. Ent. Soc. Lond., Symp.*, **2**:95-107.
- Hohorst, W. (1936) Die Begattungsbiologie der Grille, *Oecanthus pellucens* Scopoli. *Z. Morphol. Oekol. Tiere*, **32**:227-275.
- Huet, C. (1966) Etude expérimentale du développement de l'appareil genital male de *Tenebrio molitor* (Coléoptère: Tenebrionide). *O.R. Soc. Biol.*, **160**:135-139.
- Huignard, J. (1975) Anatomie et histologie des glandes annexes males au cours de la vie imaginaire chez *Acanthoscelides obtectus* Say (Coleoptera: Bruchidae). *Int. J. Insect Morphol. Embryol.*, **4**:77-88.
- Jones, J.M. (1967) A morphological study of the internal reproductive tract of male *Tenebrio molitor* L. Master's Thesis, Catholic University of America, Washington, D.C.
- Jones, J.C., and B.V. Madhukar (1976) The potency of male accessory gland material in the mosquito (*Aedes aegypti*). *Experientia*, **32**:452-453.
- Judson, L. (1967) Feeding and oviposition behavior in the mosquito *Aedes aegypti* (L) I. Preliminary studies of physiological control mechanisms. *Biol. Bull.*, **133**:369-377.
- Kafatos, F.C., J.C. Regier, G.C. Mazur, M.R. Nadel, H.M. Blau, W.H. Petri, A.R. Wyman, R.E. Gelinis, P.B. Moore, M. Paul, A. Efstratiadis, J.N. Vournakis, M.R. Goldsmith, J.R. Hunsley, B. Baker, J. Nardi, and M. Koehler (1977) The eggshell of insects: differentiation-specific proteins and the control of their synthesis and accumulation during development. In: *Results and Problems in Cell Differentiation*, Vol. 8, Biochemical Differentiation in Insect Glands. W. Beermann, ed. Springer-Verlag, Berlin, Heidelberg, New York, pp. 45-145.
- Kaulenas, M.S. (1976) Regional specialization for export protein synthesis in the male cricket accessory gland. *J. Exp. Zool.*, **195**:81-96.
- Kawasaki, H., H. Sato, and M. Suzuki (1971) Structural proteins in the egg-shell of the oriental cricket, *Gryllus mitratus*. *Biochem. J.*, **125**:495-505.
- Kerschner, T. (1913) Die Entwicklungsgeschichte des männlichen Copulation apparats von *Tenebrio molitor* L. *Zool. Jahrb., Abt. Anat.*, **36**:337-376.
- Khalifa, A. (1949) Spermatophore production in Trichoptera and some other insects. *Trans. R. Entomol. Soc. Lond.*, **100**:449-479.
- Khalifa, A. (1950a) Spermatophore production in *Blattella germanica* L. (Orthoptera: Blattellidae). *Proc. R. Entomol. Soc. Lond.*, **25**:53-61.
- Khalifa, A. (1950b) Spermatophore production in *Galleria mellonella* L. (Lepidoptera). *Proc. R. Entomol. Soc. Lond.*, **25**:33-42.
- Labine, P.A. (1964) Population biology of the butterfly *Euphydryas editha* I. Barriers to multiple insemination. *Evolution*, **18**:335-336.
- Landa, V. (1960) Origin, development and function of the spermatophore in cockchafer (*Melolontha melolontha* L.). *Acta Soc. Entomol. Cechoslov.*, **57**:297-316.
- Landa, V. (1961) Experiments with an artificial spermatophore in the cockchafer (*Melolontha melolontha* L.). *Acta Soc. Entomol. Cechoslov.*, **58**:297-301.
- Lane, N.J. (1968) The thoracic ganglia of the grasshopper, *Melanoplus differentialis*: fine structure of the perineurium and neuroglia with special reference to the intracellular distribution of phosphatases. *Z. Zellforsch.*, **86**:293-312.
- Lenep, E.W. van, A.R. Kennerson, C.G. Duck-Chong, and J.K. Pollak (1978) Fine structure of the secretion granules in the mandibular gland of echidna, *Tachyglossus aculeatus* (Monotremata). *Cytobiologie*, **18**:1-9.
- Leopold, R.A. (1976) The role of male accessory glands in insect reproduction. *Ann. Rev. Ent.*, **21**:21-43.
- Leopold, R.A. and M.E. Degrugillier (1973) Sperm penetration of housefly eggs: evidence for involvement of a female accessory secretion. *Science*, **181**:555-557.
- Locke, M. (1974) The structure and formation of the integument in insects. In: *The Physiology of Insecta*. M. Rockstein, ed. Academic Press, New York, p. 124-213.
- Loher, W., and F. Huber (1966) Nervous and endocrine control of sexual behavior in a grasshopper (*Gomphocerus rufus* L.). *Symp. Exp. Biol.*, **20**:381-400.
- Neville, A.C. (1975) *Biology of the Arthropod Cuticle*. Springer-Verlag, Berlin.
- Noirot, C., and C. Noirot-Timothee (1967) Un nouveau type de jonction intercellulaire (zonula continua) dans l'intestin moyen des Insectes. *C.R. Acad. Sci. Paris*, **264**:2796-2798.
- Noirot-Timothee, C., and C. Noirot (1966) Attache de microtubules sur la membrane cellulaire dans le tube digestif des termites. *J. Microscopie*, **5**:715-724.
- Odhiambo, T.R. (1969) The architecture of the accessory reproductive glands of the male desert locust. I. Types of glands and their secretions. *Tissue Cell*, **1**:155-182.
- Pearse, A.G.E. (1968) *Histochemistry, Theoretical and Applied*. Vol. I. J. and A. Church, Ltd, London.
- Pickford, R., A.B. Ewen, and C. Gillot (1969) Male accessory gland substances: An egg-laying stimulant in *Melanoplus sanguinipes* (F.). *Can. J. Zool.*, **47**:1199-1203.
- Poels, A. (1972) Histophysiologie des voies genitales males de *Tenebrio molitor* L. (Coleoptere: Tenebrionidae). *Ann. Soc. R. Zool., Belg.*, **102**:199-234.
- Reynolds, E.S. (1963) The use of lead citrate at high pH as an electron-opaque "stain" in electron microscopy. *J. Cell Biol.*, **17**:208-213.
- Riemann, J.G., and B.J. Thorson (1969) Effect of male accessory material on oviposition and mating by female house flies. *Ann. Entomol. Soc. Am.*, **62**:828-834.
- Riemann, J.G., and B.J. Thorson (1979a) Ultrastructure of the accessory glands of the Mediterranean flour moth. *J. Morphol.*, **159**:355-392.
- Riemann, J.G., and B.J. Thorson (1979b) Foliate and granule secreting cells in the ejaculatory duct (simplex) of the Mediterranean flour moth. *J. Ultrastruct. Res.* (in press).
- Ruby, J.R., and H.B. Canning (1978) Ultrastructure of the acinar cells in the submandibular gland of the nine-banded armadillo. *J. Morphol.*, **155**:1-18.
- Satir, P., and N.B. Gilula (1973) The fine structure of membranes and intercellular communication in insects. *Ann. Rev. Ent.*, **18**:143-166.
- Schuel, H., W.L. Wilson, J.R. Wilson, and R. Schuel (1969) Separation of intact cortical granules from homogenate of unfertilized sea urchin eggs by zonal centrifugation. *J. Histochem. Cytochem.*, **17**:703-713.
- Simões, L.C.G., A. Jurand, and S.S. Sehgal (1977) Cell differentiation during the ontogeny of larval salivary glands of the fly, *Telmatoscopus albipunctatus*. *J. Insect Physiol.*, **23**:843-854.
- Slavin, B.G., P.M. Beigelman, and S.P. Bessman (1977) Cytophysiological studies on isolated pancreatic islets *in vitro*. *Anat. Rec.*, **188**:445-452.
- Smith, D.S. (1968) *Insect Cells*. Oliver and Boyd, Edinburgh.
- Smithe, F.B. (1975) *Naturalist's Color Guide*. The American Museum of Natural History, New York.
- Spradling, A.C., and A.P. Mahowald (1979) Identification and genetic localization of mRNAs from ovarian follicle cells of *Drosophila melanogaster*. *Cell*, **16**:589-598.
- Suzuki, Y. (1977) Differentiation of the silk gland. A model

- system for the study of differential gene action. In Results and Problems of Cell Differentiation, Vol. 8, Biochemical Differentiation in Insect Glands. W. Beermann, ed. Springer-Verlag, Berlin, Heidelberg, New York, pp. 1-44.
- Takashima, Y. (1960) Studies on the ultrastructure of the cortical granules in sea urchin eggs. *Tokushima J. Exp. Med.*, 6:341-349.
- Tandler, B., and D.K. MacCallum (1972) Ultrastructure and histochemistry of the submandibular gland of the European hedgehog, *Erinaceus europaeus* L. *J. Ultrastruct. Res.*, 39:186-204.
- Terakado, T., and H. Mukai (1978) Ultrastructural studies on the formation of yolk granules in the statoblast of a fresh water Bryozoan, *Pectinatella gelatinosa*. *J. Morphol.*, 156:317-338.
- Theron, J.J., R. Biagio, A.C. Meyer, and S. Boekooi (1978a) Ultrastructural observations on the maturation and secretion of granules in atrial myocardium. *J. Mol. Cell. Cardiol.*, 10:567-572.
- Theron, J.J., R. Biagio, A.C. Meyer, S. Boekooi, and J.C. Seegers (1978b) The effect of a serotonin inhibitor on the serotonin content and ultrastructure of rat atria and ventricles with special reference to atrial granules. *Life Sci.*, 23:111-120.
- Waring, G.L., and A.P. Mahowald (1979) Identification and time of synthesis of chorion proteins in *Drosophila melanogaster*. *Cell*, 16:599-607.
- Waterhouse, D.F. (1957) Digestion in insects. *Ann. Rev. Entomol.*, 2:1-18.
- Wigglesworth, V.B. (1972) *The Principles of Insect Physiology*. Chapman and Hall, London.
- Wigglesworth, V.B. (1979) Secretory activities of plasmatocytes and oenocytoids during the moulting cycle in an insect (*Rhodnius*). *Tissue Cell*, 11:69-78.
- Zacharuk, R.Y. (1958) Structures and functions of the reproductive systems of the prairie grain wireworm, *Ctenicera aeripennis destructor* (Brown) (Coleoptera: Elateridae). *Can. J. Zool.*, 36:725-751.